Response to the review

Reviewer 1: Eric Larour

The manuscript is generally well written, and the science exposed here warrants publications, as it has strong implications in terms of significantly improving ice sheets models and providing benchmarks that can be compared against to check whether our models are capable of modeling different areas of the ice sheet, ranging from fast-flowing areas such as ice streams, to ice divides, or here BIAs.

Thank you for this positive assessment.

The only problem I have with the manuscript is the constant intertwining of content relating to the 2D flow-line model and to the 3D full-Stokes model. It is quite difficult to follow the main thread, and I am not sure the flow-line model brings much to the paper, apart from providing nice figures in Fig. 4 and 5 which do not per-se depend on the nature of the model. I am as of this writing still not clear on what the flow-line model is exactly used for compared to the 3D model. The manuscript would gain much in reorganizing to avoid this confusion.

We agree with this statement. In the first version of the paper we organized the manuscript along the chronological order of our numerical investigations, which - after a first 3-D simulation using isotropic rheology – lead us to experiments on flow-line models to capture the main features of different rheology and then back to the 3-D runs. As this, admittedly, is a source of confusion, we reorder such that we clearly distinguish between results obtained on the whole domain (3-D) and those from the flow-line model (2-D). We, nevertheless, think that keeping 2-D simulations within the article is important to show the deviation of results obtained with the flow-line in comparison the corresponding vertical intersection of full 3-D model, as earlier investigations (Grinsted et al., 2003) used such reduced models for studies of flow dynamics and the age-horizons at Scharffenbergbotnen.

Detailed remarks:

• p 3060: *Abstract: abstract is clear, concise, and to the point.*

Thanks

• *p 3061: The with respect – > With respect to snow-covered areas, lowered surface albedo of BIAs...*

Changed into: “The lower albedo of bare ice surfaces relative to ...”.

• p 3061.l16: *this is a very nice segment of the manuscript, which is very useful in* *understanding why exactly this area is of interest.*

Thank you for that feedback.

• p 3061.l09: *It would be interesting to know at this point what is meant by such models, and what is the property here that is of interest in such models that would allow for a better fit to observations. What is exactly the feature of ice flow that is not well reproduced? The ice-bridging effect? The higher-order vertical shear stresses? Is full-Stokes really needed or does a Blatter/Pattyn approach do the trick?*

This is a good point and we want to emphasize, that the main reason why we apply a full Stokes model simply is, because we have one (=Elmer/Ice) at hand and hence do not have to worry about errors that might have been introduced by a certain approximation to the full set of stresses. Motivation for such a choice may be given by the fact that

1. The Scharffenbergbotnen valley glacier at some places is equally deep as wide, i.e., the aspect ratio is close to unity.
2. As we describe in the paper to be the reason for the interest in this area, the almost horizontally aligned isochrones at the surface of the ablation zone imply at least similar velocities in vertical than horizontal, which renders assumptions based on shallowness of the flow to some extent questionable.
3. Anisotropy is easier to be implemented in a full stress model and an anisotropy model – which in itself is a demanding task to develop - already existed.

Applicability of Blatter-Pattyn, for instance, might be sufficient with respect to the anyhow big errors in the available measurements, but it is not within the scope of that paper to prove this.

• p 3061: *it would be nice to refer to Fig. 1, as modified per remarks below, i.e. in order to give the reader a clear idea of where Scharffenbergbotnen is located.*

We inserted a reference to Fig. 1., where we add a sketch of Antarctica showing the location of SBB and one satellite picture in order to help the reader identify the location of the site.

• p 3062.l27: *from the North-West and the West as specific locations?*

North-western and western was meant relative to the valley. We do not completely understand what the reviewer demanded and hope that the new formulation “from the wide north-northwestern entrance” in combination with a stake position suffices.

• p3064.l18: *I’m not sure this squares off with the introduction, which strongly argued for full-Stokes higher-order models when here the authors are now discussing flow-line modeling. Such models have serious limitations, even in full-Stokes mode. This should be discussed here, or the rationale for using such models explained from the get go.*

We agree with the reviewer that flow-line models have restrictions, simply implied by the reduced ability to account for the complex geometry and of course also in representing effects of lateral stress components. As mentioned before, we explicitly want to keep some of these results in the paper in order to demonstrate this, as flow-line models have been used for earlier studies on SBB.

• p3064.l29: *I have some reservations here as to the rationale of flow-line modeling. In* *a situation where the ice essentially stagnates, and where the authors are trying to explain discrepancies in strong vertical velocities, it would seem more natural to carry out a full-scale basin model. Here, a mistake made in the choice of the flow line will result in under or over estimation of lateral shear stresses, resulting in under or over estimation of the backstress component of the ice flow.*

For exactly that reason we performed the 3-D simulations. The clear emphasis on 3-D simulations should now be more obvious in the new version of the paper. To explain a little bit our choice to deploy flow-line models: flow-line models helped us to understand the principle consequences induced by the altered rheology and were extremely useful to quickly find suitable setups that produce correct trends.

• p3065.l6: "*Now we think": this goes to my previous remark. It would seem that something more tangible should be at the origin of the flow-line identification, as it is such a critical step if the use of a collapsed formulation is to be realistic. At least, if computational requirements are an issue here, the full-Stokes 3D model could be used in diagnostic mode to correctly capture the flow-line direction, then used to constrain the model setup for the flow-line model. This would ensure a realistic pick for the flow-line path, consistent with the assumptions of the flow-line full-Stokes model.*

Again, the flow-line studies were not intended to produce quantitative results (in the strict sense neither the 3-D), but rather to work out a trend. We took care to clearer state this in our new version and put the focus on the 3-D cases.

• p3065.l11: *the authors should discuss the geothermal heat flux values, and at least run identical configurations with geothermal heat fluxes from Maule et al. 2005, or discuss the implications of not knowing the geothermal heat flux accurately.*

Also by request of the other reviewer, we have added information that will demonstrate the relative (un-) importance of the value of the geothermal heatflux.

• p3066.l17:20: *very nice segment which was clearly needed here.*

Again, thanks for the positive feedback.

• p3067.l9: *the body of work from Durand et al on this should probably be cited.*

We include Patterson's monograph to point to the unreferenced Arrhenius dependency as well as a reference to Duval (corrected from Durand after personal communication with the reviewer) in the context of anisotropy of ice and hope that this is an acceptable solution.

• p3067.l17: *I don't understand why this is done. In a code like Elmer, these terms are already captured, so why neglect them, when this could lead to some modifications in the results. There is no computational impact to adding these terms in the computation of the thermal regime, so why not play it on the safe side, and include them?*

The reviewer is correct in that sense, that the additional computational load would have been negligible. We evaluated these terms for one instance and they were so small that they had no influence. The picture (right) shows a comparison of the resulting temperature distributions between the flow line model temperature distribution for a run with and without strain heating. Even on a point-by-point value comparison the differences are small fractions of a degree, such that we with absolute confidence can claim that strain heat does not alter the results.

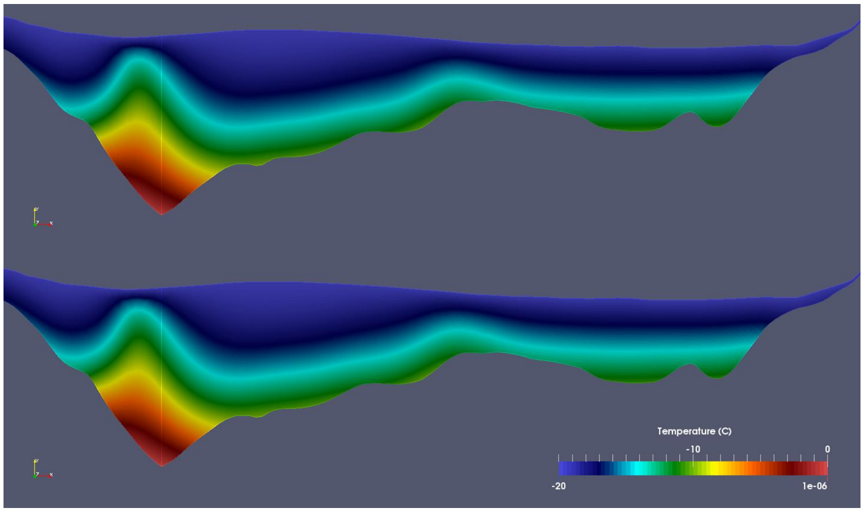

• p3068.l6: *correspond with – > corresponds to ?*

done

• p3071.l25: *is pre-conditioned – > are pre-conditioned*

done

• p3072.l1: *some details such as number of iterations in the Picard for each model (thermal and mechanical) as well as the overall model would be nice to have. Were there also locations where convergence could not be reached, such as freeze-on or hot-spots that osciallate through time and never reach convergence (zigzagging)?*

The maximum number of needed Piccard iterations (for the vertical single maximum fabric case) was 30. As only dealing with diagnostic runs that only lasted for about half an hour, we did not optimize for computational performance, but simply ensured that the result was converged. There are no real "hot-spots" (we assume you mean areas of temperate base) that produced any feedback of oscillatory behavior. As a matter of fact, caused by the relatively cold surface and the, compared to usual ice-sheet dimensions, moderate ice thickness the temperate base areas are limited to a small domain in the outer part of the valley, where the ice is about 1000m thick.

• p3073.l11: *I would surmise that another hypothesis could be that the isochrones would be better interpreted were they carried out with a basin-wide model, in 3D. If the flow line is not correctly calibrated, the flowline will cross isochrones from other flow-lines, resulting in a bad interpretation of the age record of this particular basin. This really needs to be addressed in the current manuscript I believe.*

We agree. We shift the focus also for the vertical cuts to present the results of the 3-D model output.

• p3073: *I would like to strike my comment above, as I now realize that a full 3D model was indeed carried out. This is confusing, as I was truly under the impression, up to*

5.1, that a full-Stokes flow-line model was what was called the 3D model. I would urge the authors to make the distinction clearer, so as to avoid similar confusion as I went through here. I now also don't understand why a flow-line model is used, if a 3D full-Stokes model was also used in 5.1.

See our earlier explanations on why we have 2-D model results. We repeatedly agree that these results in comparison to the full 3-D results got too much attention in the first version of the paper and hence we re-order the results and their presentation.

• p3075.l9: *shown in Fig. 8?*

Indeed, this is depicted in Fig. 8 rather than 7 – corrected this. Mind that we introduced two new figures and changed others, such that numbering of Figures has changed throughout the whole paper.

The figures are generally clear and self-explanatory, except for Fig 1:

• Fig. 1*: it would be nice to have an idea of where Scharffenbergbotnen is, I would suggest adding an inset to clearly define the area being studied. Fig. 1 is also overall very cluttered, and quite hard to read. I would suggest splitting velocity and age, so as to make two frames maybe?*

We worked over that issue and split Fig 1 into the suggested 2 parts.

Reviewer 2: Shin Sugiyama

1. General comments

This paper presents numerical modeling of ice flow conditions of the blue ice area at Scharffenbergbotnen. Modeled ice flow fields are used to compute ice age distributions over the surface and the results were compared with field data. Because the model results did not show reasonable agreement with observed ice velocity and age, additional experiments were performed with prescribed anisotropic ice fabrics. As a result of these experiments, the authors concluded that ice anisotropy plays a key role in the ice flow regime and ice age distributions in the studied region.

This is an interesting and valuable work which applies a "state-of-the-art" ice flow model to a very complex ice flow field in Antarctica. The Scharffenbergbotnen is a deep and narrow valley surrounded by nunataks, where ice flows into the valley, emerges to the surface, and forms a blue ice area. The authors employed a full Stokes high resolution model (Elmer/Ice), which is able to take into account higher order stress terms arise from complex bed geometry. Relatively abundant field data are available in the studied region and they are used for the validation of the modeling. Such approach is useful *for testing the performance of the latest modeling techniques and also for planning field measurements and sampling in the future. The first author has been leading the development of the Elmer/Ice model and working on many other glaciers using the same model. Thus, the modeling results are thought to be reliable.*

Because of the reasons above, the presented work meets the interests of the journal readers and details are beneficial for those engaged in this field of cryosphere science. The manuscript is generally well written in the introduction and methodology sections. In my opinion, however, interpretations and discussions on the modeling results are not sufficient in the present form. Specifically, I suggest the authors to compare the results with field data more carefully and discuss other possible factors missing in the model. Figures are nicely prepared, except for several points which should be revised for clearer presentation.

Here, I provide several concerns, specific comments to each part of the text, and technical corrections. I encourage the authors to improve the manuscript, considering the comments listed below.

We thank the reviewer for the – in our view – generally positive statement and his very detailed comments on the paper.

We try to address the concerns on the interpretation and representation of the obtained results in our revised version of the paper.

2. Major concerns

(1) Comparison of the modeling results with field data

Computed ice velocity and age are compared with field observations and ice core data. The authors concluded that the isotropic experiment was not able to reproduce the observations, whereas the results of the anisotropic experiments showed sufficiently good agreement with the observations. However, these comparisons were not performed in a quantitative manner. Figures 2, 3, 6 and 7 are the basis of their argument, but quantitative analyses were not performed. Because the authors have the details of the velocity and age data (Tables 1 and 2), it is not difficult to compare the data one by one to compute statistical values. Because errors are expected to be large in the ice age data, the comparison should be made more carefully with consideration of error bars. Scattered plots of computed and field data with error bars may be helpful for the readers to understand how much the modeling results agree/disagree with the field data.

We agree with the reviewer that adding comparison between the measured and computed variable values adds quality to the paper and come after that request by adding computed values of velocities to table 2 and a new table 3 with mass balance comparisons. To go into a detailed statistical analysis is difficult in that sense, that we do not consider the computed results to be interpreted in a quantitative way. Even more, the age distribution is a field that strongly depends on the initial distribution of the age at the LGM and the temporal evolution of the thinning inside the valley, of which we do not have any detailed information. The errors for the measured ages are anyhow given in Table 1, and as comes clear from that, all, but two measurements show a large error. Hence, matching ages with our simulation simply by the quality of the measurements is a less fruitful task than matching velocities (by magnitude and direction).

(2) Interpretations of the insufficient results from the isotropic model

The authors concluded that anisotropic ice rheology is the reason why isotropic model failed to reproduce the observed ice velocity and age. I found this argument is too strong as compared to the evidence provided in this paper. The agreement with the field data was better in the anisotropic experiments. However, the single maximum ice everywhere in the glacier is a highly unlikely assumption, and thus it also implies the field data are not reproduced by a likely anisotropy distribution. I understand the assumption used for Figure 7a is a more realistic assumption, but the results disagree with the data. The authors state that other sensitivity tests were performed by tuning enhancement factor, surface temperature, and geothermal heat flux, but their results are not shown. This is pity as I expected changes in ice temperature might have a large influence on the results. I also suspect the uncertainty in the bed geometry affects the englacial velocity field. Surface elevation change in the past is also relevant to the ice age. Old ice near the bed might have emerged to the surface after the change in the surface elevation. Additional experiments with 100 m thicker ice may give insights into such possibilities. These are all my speculations, but still possible interpretations. I encourage the authors to perform and show the results of sensitivity tests by changing parameters possibly influence the ice velocity and age. Unless strong evidence is shown, I suggest the author to be modest about the conclusion. It is interesting enough to propose the anisotropy as one of the important factors in the studied region. Listing other possible factors is also beneficial for those work on similar problems in the future.

We remain with our position that – by excluding all other possibilities – a pronounced fabric at the domain of the BIA is the most likely remaining explanation of the observed flow field. In order to underline this, we present statistics gathered on the inner BIA from different variations of the isotropic runs, using different thermodynamic boundary values (geothermal heatflux, surface temperature) as well as a run including manipulation of the enhancement factor. Those findings confirm that an anisotropic rheology is needed to change the behavior of the flow differently in horizontal and vertical directions (what is necessary accordingly to our observations on surface velocities, ages and surface mass balance). All changes applied to parameterization of isotropic rheology did not lead to such an effect.

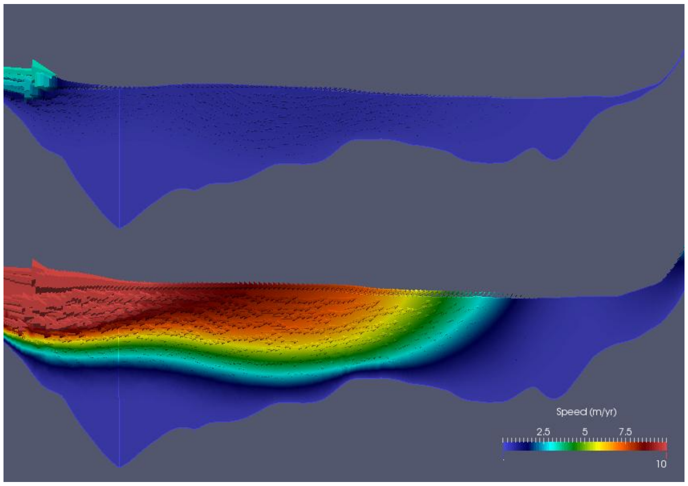

Diagnostic runs with a different surface geometry (the suggested +100m geometry) in our opinion are of limited use, as they do not include any information on the lowering. We already explained in the paper, why it is currently impossible to perform transient simulations starting from the LGM. Hence we excluded this information from the paper. We only here demonstrate the result (left) of an isotropic run done on a flow-line model that uses a by 200m (not 100m) exaggerated thickness. To no surprise (as they scale with the 4th power of the thickness), velocities (bottom) are way larger than in the present day configuration (top).

Inconsistent bed geometry usually manifests itself in locally unrealistically large velocities. As mentioned, we did an initial relaxation run (i.e., prognostic run with a freely evolving surface) that did not show any spots with artificially high velocities. From this we concluded that eventual errors in bedrock geometry did not affect the over-all flow pattern.

(3) Interpretation of the results

The results presented in the section 5 contain interesting and important information related to the ice flow and temperature regime in the blue ice area. Unfortunately, the details of the modeling results are not explained very well except for surface horizontal velocity and ice age. I suppose many readers, including me, are interested in other aspect of the results. For example, vertical component of the surface velocity can be compared with surface mass balance measured in this region. Englacial temperature field under the influence of complex ice flow regime and bed geometry is also worthy of discussion. Ice flow field obtained by the anisotropic fabric also needs more interpretations because the influence of anisotropy is not intuitive. Single maximum fabric resists to deformation to one direction (or stress regime), but it deforms more to the other directions (or stress regime). Significantly slower ice motion obtained with the anisotropic fabric can be discussed with englacial stress and strain regimes.

We took efforts to elaborate on a comparison of computational results with measured data. In particular, we introduced statistics taken over the inner BIA that clearly show that only anisotropic rheology can produce the trends in directional ice velocities that are needed to match observed data. We also have a comparison between measured and computed surface mass balance, which even stronger underlines the significantly better match of data in case of highly anisotropic rheology. The effect of changing thermal boundary conditions (and consequently changing englacial temperatures) is depicted in a statistics that compares the impact on velocities by changing parameters in an isotropic simulation.

3. Specific comments and Technical corrections

Title: » This title gives a strong impression about the role of the anisotropy at Scharf-

fenbergbotnen. In my opinion, a more general title something like "Numerical modeling

of ice velocity and age distribution at Scharffenbergbotnen blue ice area" suites the

paper as it stands.

The referee is correct in what he thinks the title and the paper are about. We do not see that the paper needs a change of title since it is exactly the anisotropy that is the key point here.

- page 3060, line 10: *» . . . and too slow vertical ones "obtained in the model"*

  Changed into: "vertical ones in simulations".

- page 3060, line 15: *. . . both two-dimensional and three dimensional flow models. » Use of the two models should be mentioned earlier?*

  This issue has been solved by shifting the focus of the paper almost entirely on the 3-D runs.

- page 3061, line 11: *The with respect to . . . » Something wrong?*

  Changed into: "The lower albedo of bare ice surfaces relative to snow covered areas enhances ablation in BIAs".

- page 3063, line 4: *the outside ice-sheet » Not clear where it is.*

  Changed into: "the ice-sheet outside the valley".

- page 3063, line 6-8: *As the elevation . . . » Is this a well-established idea? Any citation?*

  We added reference to Hättestrand, C. and Johansen. Many other authors we do not cite also show this.

- page 3063,line 14: *...increases towards the center of the valley. . . » Increases from where to the center of the valley? What do you mean by "the center of the valley"?*
  Changed into: "generally increases from the flanks of the nunataks surrounding the valley towards the center of the valley".

- page 3063, line 25 *complete slate-blue » This is very difficult to find. Text labeling on the map is helpful.*

  Also by request of the other reviewer, we split the old Figure 1 into two separate ones, from which positions and annotations should be easier to spot.

- page 3063, line 29: *. . . including the band . . . » What is "the band"?*
  We elaborated: " including relatively darker band (orange feature in Fig. 2) in the ice at position b15".

- page 3064, line 9-10: *. . . before the full impact of . . .. » Not clear what is meant.*

  In situ production C14 refers to production of C14 by cosmic rays with nuclei of atmospheric gases in the air bubbles in the upper meters of the ice (the reference cited describes this process). This means that the C14 measurement will not give a reliable age as there is an assumption in radio-dating that the reservoir of C14 was fixed at the date of snow precipitation.

- page 3064, line 27: *to follow the deepest surface incline path » Do you mean something like "along the direction of the maximum inclination"?*

  No, this sentence was confusing and is now deleted.

- page 3065, line 16: *varied by about -9 to +3K » citation?*

  We inserted a reference (Sato and Greve, 2012) – the corresponding used temperature curve for the very location we got from one of the authors looks like this (temperature deviation from present vs. years relative to present date).

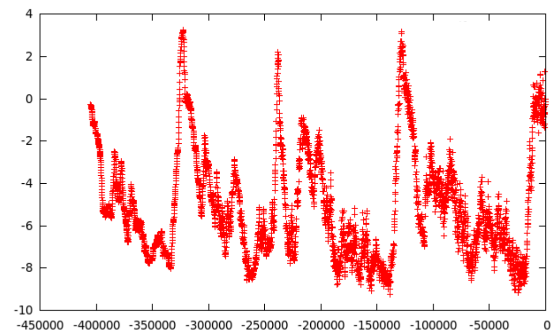

- page 3067, line 3: *collinearly » It sounds strange to me because stress-strain relation-ship is nonlinear in Glen's flow law.*

  Collinearly in our view is correct, as it means that the tensor on the l.h.s. is aligned with the one on the r.h.s. – this is valid despite the highly non-linear relation of the scalar viscosity.

- page 3067, line 7: *» second invariant of the strain rate "tensor".*

  Corrected as requested.

- page 3067, line 22: *Martin and Gudmundsson (2012) » The publication year disagree with the reference list.*

  Corrected.

- page 3069, line 18-19: *mean average temperature » What do you mean?*

  Rephrased to: "present annual mean temperature".

- page 3070, line 2-3: *. . . pointing against the outward facing surface normal Eq. (13) »pointing into the glacier*

  Changed as suggested.

- page 3070, line 7: *freeze-on condition for . . ... all over this boundary. » fixed boundary condition (u=0) at the bed?*

  Rephrased to: "This allows for setting a fixed boundary condition, $\vec{u}=\vec{0}$, for the velocity at the bedrock."

- page 3071, line 3: *By the nature of the problem, » This is not clear.*

  Rephrased to: "As only limited geomorphological information on LGM geometry is available (Näslund et al., 2000; Hattestrand and Johansen, 2005)".

- page 3071, line 3: *. . . the first of these items are . . . » . . . the first of these items is . . .?*

  Rephrased to: "the first two of these items are".

- page 3071, line 7: *» Delete one of "the".*

  done

- page 3071, line 13: *» Delete "and"?*

  We changed the “and” into “an”.

- page 3072, line 4: *4.1 Prescribed anisotropy » It’s odd to have only one subsection in section 4.*

  We removed the subsection.

- page 3072, line 12: *vertical fl30 depth » Not clear to me. Do you mean somewhat "vertical displacement from the initial deposition on the surface"?*

  Replaced with: “the distance from the free surface”.

- page 3074: *5.2 Simulations using 2-D flow line model » Figure 4 and 5 show nice plots, but they are not well explained in this section. Each panel is even not referred in the text (Figure 4a, Figure 4b, . . .). I would like to read more details about the results by pointing out specific part of the figures. For example, the authors state that "they now even underestimate the observed flow speeds in places." (line 14-15), but not clear where and how much the results underestimate the observations .*

  Upon suggestion by the first reviewer, we rearranged the presentation of results and also the annotations, hoping that the new version also eliminates these correctly raised issues and deepened their interpretation and discussion.

- page 3074, line 7: *naturally, as at the surface . . . » Why do you think it’s natural? Usually, deformation near the bed is more important than that near the surface.*

  The reviewer is right – it is not in order to make such a general statement – it rather seems to apply to the specific geometry at SBB, which certainly differs tremendously from a general glacier/ice sheet type of flow, where surface velocities are more or less determined by near-bed deformation and sliding. We anyhow modified this part of the text on request by the first reviewer.

- page 3074, line 9: *much flatter » Not clear.*

  Indeed, this is unfortunately formulated. We meant to say: “more horizontally aligned”.

- page 3074, line 11: *. . . more towards the lower end of the valley . . . » Do you mean "down the valley"?*

  Yes, correctly anticipated by the reviewer and not clearly formulated by the author.

- page 3074: *5.3 Simulations using prescribed fabrics in 3-D » I have the same impression as I wrote above for the section 5.2. I suggest the author to explain the results more in detail and compare them with the field data in a quantitative manner. For example, the paragraph starting from line 25 can be improved by giving numbers instead of "slightly lower" or "slightly too slow".*

  We hope to comply by inserting the values for the computed velocities and get into more details in their discussion.

- page 3075, line 9: *Fig. 7 » Fig. 8?*

  This indeed was wrong.

- page 3075, line 12-13: *(as stream lines are not expected to cross surface moraines) » Why do you expect not? Why does the model compute such an unrealistic result?*

  Answer to first question: Moraines have to be aligned with stream lines (else material would be advected away from them), which naturally implies that streamlines do not cross.

Answer to second question: The model produces such an unrealistic solution because of the wrong (isotropic) rheology. And that discrepancy remains even if we vary several parameters (temperature, heatflux, enhancement factor) for the isotropic case.

- page 3075, line 17-19: *i.e., the resulting physical time . . . » I think this is unnecessary rewarding.*

  As we interpret this comment by the reviewer, there is a misunderstanding caused from our side by a sloppy formulation of this sentence. What we meant to say is that the values obtained with the Runge-Kutta method changes significantly between isotropic and single-maximum setup. We are reformulating this in the new version to: “the travel time of a particle as a result from the Runge-Kutta method to advect a particle from the surface along the stream-line back to that particular position“.

- page 3076, line 26: *Fig. 7 » Fig. 8*

  This indeed was wrong, as before.

- page 3077, line 12-14: *Strong fabric development . . . » These two citations report ice fabrics at very different conditions from the study site of this paper. They are not convincing evidence of strong anisotropy near the surface of blue ice area.*

  We agree with the reviewer that the measurements of ice-fabric are not from a BIA but, to our knowledge, there are no measurements of ice-fabric over BIAs. However, every measurement available of ice-fabric shows strong fabric development in shallow ice (e.g., Svensson 2007 and Matsukoa 2012). This is explained by previous modelling results, that show that under compression, extension and shear, flow-induced anisotropy develops in a fraction of the advection time-scale, ice-thickness divided by vertical velocity, that is a fraction of tens of thousands of years in SBB (Martín and Gudmundsson, 2012). We also agree that the conditions of compression, extension and shear in Martin (2012) are not identical to the conditions in SBB BIA, but our results support the idea that fabric evolve as rapidly in a BIA as in other areas with different ice-flow characteristics. We have rewritten the paragraph to make this important point clearer.

- page 3077, line 17-19: *Even if . . . » I cannot follow this argument. Why can it evolve rapidly?*

  We have rewritten the paragraph to more clearly elaborate this argument.

- page 3078, line 3*: . . . non-linear evolution of the valley . . . » What kind of evolution?*

  We rephrased: “an in time non-linear thinning of the surface inside the valley”.

- page 3078, line 25-26: *This suggests that the BIA was formed . . . » I cannot follow this argument. Which part of the text discusses this point?*

  This is a conclusion from the three facts mentioned in the text: in the simulation, the age-field of the ice at surface never is in a steady state, it is about as old as the simulation time (+ the initial condition) itself and the measurement at this part of the glacier do not reveal ages above 15ka. These three constraints mean that the ablation at the position of the BIA has started sometimes between LGM and present day – with the exact timing of course being unknown, as we do not know the history of the lowering.

- page 3080, line 12: *» Please check the publication year, 2005 or 2003?*

  This is correct, because 2005 is not a date, but rather an article number.

- Figure 1: *» This plot is beautifully drawn, but very difficult to read when it is printed. It should be large enough to read the details when it appears in the final paper.*

We agree that this is a too busy sketch. Also on request by the other reviewer, we split this figure into 2 in order to help the reader to tell the trees from the forest.

- Figure 4 and 5: *» What are the three color dots at the upper right corner of each panel?*

  The – admittedly confusing - three dots were a legend automatically added by the plotting program and have been taken out from the new versions.

- Figure 5a-c: *» I understand these are results of the 2D model. If yes, the texts at the upper right corner are not correct.*

  Indeed, the annotations in the first three were wrong. We anyhow changed those figures.

- Figure 5 caption: *Comparison of absolute velocity . . . Comparison of absolute "horizontal" velocity . .*

  Corrected.

- Figure 8: *This plot is also difficult to read when it is printed. It should be very large or needs some modifications. The numbers for the color code "-5000 -4e+4 -2e+4 0" should be "-5000 -4000 –3000"*

  Three-dimensional post-processing of an irregular topography/flow on paper is a difficult task, but we hopefully improved the appearance of this figure in the new version of the article by rearranging it and hereby increasing the size as well as by enhancing the contrast. The numbering has been changed according to the reviewer's request.

References

Grinsted, A., Moore, J., Spikes, V. B., and Sinisalo, A.: Dating Antarctic blue ice areas using a novel ice flow model, Geophys. Res. Lett., 30, 2005, doi:10.1029/2003GL017957, 2003.

Svensson, A., Durand, G., Mathiesen, J., Persson, A., and Dahl-Jensen, D.: Texture of the Upper 1000 m in the GRIP and North GRIP Ice Cores, in Physics of Ice Core Records II: Papers collected after the 2nd International Workshop on Physics of Ice Core Records, held in Sapporo, edited by: Hondoh, T., Japan, 2-6 February 2007, 2007.

Matsuoka, K., Power, D., Fujita, S., and Raymond, C. F.: Rapid development of anisotropic ice-crystal-alignment fabrics inferred from englacial radar polarimetry, central West Antarctica, J. Geophys. Res., 117, F03029, doi:10.1029/2012JF002440, 2012.

Martín, C. and Gudmundsson, G. H.: Effects of nonlinear rheology, temperature and anisotropy on the relationship between age and depth at ice divides, The Cryosphere, 6, 1221-1229, doi:10.5194/tc-6-1221-2012, 2012.

Sato, T., and Greve, R.: Sensitivity experiments for the Antarctic ice sheet with varied sub-ice-shelf melting rates, Ann. Glaciol., 53(60), 221—228, doi:10.3189/2012AoG60A042, 2012

Manuscript prepared for The Cryosphere Discuss.
with version 3.5 of the LaTeX class copernicus_discussions.cls.
Date: 12 December 2013

Influence of anisotropy on velocity and age distribution at Scharffenbergbotnen blue ice area

T. Zwinger[1], **M. Schäfer**[2], **C. Martín**[3], **and J. C. Moore**[4,2,5]

[1]CSC-IT Center for Science Ltd., Espoo, Finland
[2]Arctic Centre, University of Lapland, Rovaniemi, Finland
[3]British Antarctic Survey, Cambridge, UK
[4]College of Global Change and Earth System Science, Beijing Normal University, Beijing, China
[5]Department of Earth Sciences, Program for Air, Water and Landscape Sciences, Uppsala University, Uppsala, Sweden

Correspondence to: T. Zwinger (zwinger@csc.fi)

Abstract

We use a full-Stokes thermo-mechanically coupled ice-flow model to study the dynamics of the glacier inside Scharffenbergbotnen valley, Dronning Maud Land, Antarctica. The domain encompasses a high accumulation rate region and, downstream a sublimation-dominated bare ice ablation area. The ablation ice area is notable for having old ice at its surface since the vertical velocity is upwards, and horizontal velocities are almost stagnant there. We compare the model simulation with field observations of velocities and the age distribution of the surface ice. No satisfactory match using an isotropic flow law could be found because of too high vertical velocities and much too high horizontal ones in simulations despite varying enhancement factor, geothermal heat flux and surface temperatures over large ranges. However, the existence of a pronounced ice fabric may explain the observed present day surface velocity and mass balance distribution in the inner Scharffenbergbotnen blue ice area. Near absence of data on the temporal evolution of Scharffenbergbotnen since the Late Glacial Maximum necessitates exploration of the impact of anisotropy using prescribed ice fabrics: isotropic, single maximum, and linear variation with depth, in both two-dimensional and three-dimensional flow models. The realistic velocity field simulated with a non-collinear orthotropic flow law, however produced surface ages in significant disagreement with the few reliable age measurements and suggests that the age field is not in a steady state and that the present distribution is a result of a flow reorganization at about 15 000 yr BP. In order to fully understand the surface age distribution a transient simulation starting from the Late Glacial Maximum including the correct initial conditions for geometry, age, fabric and temperature distribution would be needed. This is the first time that the importance of anisotropy has been demonstrated in the ice dynamics of a blue ice area and demonstrates the need to understand ice flow in order to better interpret archives of ancient ice for paleoclimate research.

1 Introduction

Blue ice areas (BIAs) make up about 1 % of the surface area of Antarctica (Bintanja, 1999). They are usually formed where removal of snow fall by wind exceeds precipitation (Crary and Wilson, 1961), though low lying regions allow surface melt to be the dominant process. The Scharffenbergbotnen BIA (see Fig. 1), in common with most BIAs, is located in a region where wind speeds are higher than normal for Antarctica. High winds are in general because of steep gradients promoting katabatic flows, or in mountain areas where local wind fields determined by the geometry of mountains and ice surface lead to accelerated flow (Takahashi et al., 1992). Ice flow then brings deeper ice to the surface exposing aged solid blue ice (Naruse and Hashimoto, 1982; Whillans and Cassidy, 1983; Azuma et al., 1985; Bintanja, 1999). The lower albedo of bare ice surfaces relative to snow covered areas enhances ablation in BIAs (Bintanja and Reijmer, 2001). Consequently, isochrones are inclined relative to the surface – from sub-horizontal near the equilibrium line to near vertical at the stagnant ends of the valley (Naruse and Hashimoto, 1982; Whillans and Cassidy, 1983). This makes BIAs an ideal location to obtain "horizontal ice cores" – that is collecting samples for analysis along a shallow surface trench rather than traditional deep drilling – which may contain a record of climate record spanning the Holocene and perhaps longer (Moore et al., 2006; Sinisalo and Moore, 2010). Presently, however the problems in dating and interpreting climate records from horizontal ice cores have largely precluded their usefulness as climate archives (Sinisalo and Moore, 2010). Chief among these difficulties is an understanding of the long term stability of the blue ice as the surrounding ice sheet changes through a glacial cycle.

Ice sheet elevation changes at the glacial termination are likely to have been most pronounced in the nunatak areas, such as Scharffenbergbotnen, a few hundred kilometres from the coast (Pattyn and Decleir, 1998), since this is the transitional area between cold-based and warm-based ice flow. The surface of the major part of the East Antarctic plateau ice sheet may have been about 100 m lower in the last glacial than at present (Jouzel et al., 1989; Pattyn, 1999; Ritz et al., 2001). In contrast, the surface elevation at the margins of the plateau, may have been hundreds of meters higher (Näslund et al., 2000; Hättestrand and Johansen, 2005).

Understanding the present day ice dynamics of BIAs is challenging. Several attempts have been made using simplified flow models constrained by limited data (Naruse and Hashimoto, 1982; Azuma et al., 1985; Van Roijen, 1996; Grinsted et al., 2003; Sinisalo et al., 2004; Moore et al., 2006; Sinisalo et al., 2007). However the complex geometry, usually including large ice thickness variations along the blue ice field, suggests that a three dimensional, higher order or full-Stokes model is needed to produce realistic ice flow simulations. Scharffenbergbotnen is the best studied BIA with a long history of observations including ice depth, surface velocities, mass balance, ice dating, ice temperature measurements, and both vertical and horizontal ice core archives of ice chemistry and water isotopes (the data sets are summarized in Sinisalo and Moore, 2010). Hence this BIA is a suitable test bed for numerical simulation using advanced flow modeling, which could provide insights on the dynamical evolution of the region since the last glacial.

After presenting the input data in Sect. 2, we introduce our model and the chosen initial and boundary conditions (Sect. 3). The simulation setup as well as the basic concepts of the applied anisotropic rheology follow in Sect. 4. The different approaches in terms of simulations are presented in Sect. 5, discussed in detail in Sect. 6, from which the conclusions (Sect. 7) with respect to the dynamics and age distribution at Scharffenbergbotnen are deduced.

2 Study area: Heimefrontfjella, Scharffenbergbotnen

Scharffenbergbotnen (SBB), north-west Sivorgfjella (74° S, 11° W, 1200 m a.s.l.), is a closed glaciated valley with inflow from the surrounding ice-sheet. The head of the valley acts as a dam on the main flow. There are two separate BIAs (light-gray in Fig. 1) in the valley, however this work focuses on the innermost one. Today, ice flows into the valley mainly from the wide north-northwestern entrance, generally with an eastward directed flow direction (see stake 6 in Fig. 1) and, to a very limited extent, over the mountains in an ice-fall at the eastern end of the valley (close to stake 19 in Fig. 1). Geomorphological evidence (Hättestrand and Johansen, 2005) suggests that during the Late Glacial Maximum (LGM) the ice surface in the valley was 200–250 m higher than today, while the ice-sheet outside the valley (i.e., outside the area confined by the nunataks) was only 50–150 m higher. The LGM ice sheet was able to overflow some of the passes along the valley walls and ice entered the valley from several more locations than today. As the elevation of the surrounding ice-sheet decreased after the LGM (e.g., Hättestrand and Johansen, 2005), the ice overflow became insignificant and the ice flow inside the valley decoupled from the main ice sheet flow.

A geological map of the Scharffenbergbotnen area is available from aerial photogrammetric surveys (1993, scale 1 : 25000) as is a digital elevation model of the surface (100 m resolution) based on airborne surveys in 1985/86 over the whole Heimefrontfjella area (both ©Bundesamt für Kartographie und Geodäsie, Frankfurt am Main, http://www.bkg.bund.de). Ice thickness data (100 m resolution) comes from a radio-echo sounding campaign in 1987/88 and generally increases from the flanks of the nunataks surrounding the valley towards the center of the valley but with a maximum thickness of 1050 m at the north-western entrance (Herzfeld and Holmlund, 1990).

Several ice-cores have been drilled in the area that provide data on the age of the near-surface ice. A 52 m long vertical core was drilled in summer 1997/98 in the inner part of the valley (V in Fig. 1). The uppermost 45 m section has been dated to 10500 (+700/−300) calendar years BP (van der Kemp et al., 2002), i.e. age calibrated for atmospheric ^{14}C variations. A 100 m horizontal ice-core (the surface of the ice was sampled along a trench) was collected further upstreams in 2003/04 (at H in Fig. 2). The middle part of this ice core was dated to 4426 ± 215 calendar years BP (Sinisalo and Moore, 2010). A longer horizontal core (2.7 km) was collected in 2006/07 (the complete slate-blue line in Fig. 2).

The age of the ice has been estimated at several locations (Table 1). The most reliable ages are from the ^{14}C concentration in carbonaceous particles from ice core samples (Jenk et al., 2006), but only one location (Point H) has been dated (Sinisalo and Moore (2010), Table 1, Fig. 2). Other locations were sampled, including the relatively darker band (orange feature in Fig. 2) in the ice at position b15, but no other samples contained enough carbon to produce a reliable date. Van Roijen (1996) developed a method for dating blue ice by measuring ^{14}C concentration in air trapped in the ice. In Van Roijen's method, ^{14}C depth profiles in blue ice are translated into carbon ages with a correction made for ^{14}C produced in situ, requiring an ice core to be analysed to about 50 m depth, and that results in the age at Point V, Table 1. Additional measurements are available from ^{14}C analysis in 10 other locations, see Fig. 2 (numbered empty pentagons). These ^{14}C ages had large uncertainties of up to several thousands of years (Van Roijen, 1996) since they were collected from shallow ice cores before the full impact of in situ ^{14}C production was appreciated (van der Kemp et al., 2002). The results of the ^{14}C measurements from the shallow ice cores (Van Roijen, 1996) have been corrected for atmospheric ^{14}C variations and calibrated to calendar ages using OxCal, an online calibration tool (http://c14.arch.ox.ac.uk). The errors given in Table 1 correspond to the standard deviations given by the calibration. Since these measurements are much less reliable than the two measurements obtained at V and H, they are only used for approximate age estimation.

In Sect. 5.3 we introduce a flow line model to reduce the full three dimensional solution complexity and to study principal influences from anisotropic rheology. The flow line was designed to coincide with the longer horizontal ice core (see Fig. 2). Inspection of aerial photos and maps, together with in-situ observations of the blue ice led to identification of a possible flow line on the valley. The main features used to identify this flow line were the visible bands on the ice surface (see e.g. Sinisalo and Moore (2010) – and several are also visible on the geological orthophoto map). We selected the route so that it passed through the apex of these curving structures as we supposed the ice velocity was fastest along those. The flow line terminated in the inner valley at a broad (3 m wide) band of dark colored ice that was about 1 m above the surrounding ice, and which we interpret as the confluence of the ice flow from the main entrance to the valley and the much smaller inflow from the ice fall. This convergent flow maintains a higher ice elevation on the band despite being subject to enhanced ablation due to its low albedo. The flow line defined the sampling location of the horizontal ice core. Note that this flow line is different from our previously suggested flow line (Grinsted et al., 2003), when we believed that flow originated mainly outside the valley for the inner blue ice region. Now we think that the main source of ice for the northwest part of the inner BIA is the snow accumulation region between the two BIAs – east of stake 4 north of stake 22 (see Fig. 1) – which has an especially high accumulation rate region near the north-east valley wall.

A geothermal heat flux of $q_{\text{geo}} = 60\,\mathrm{mW\,m^{-2}}$ was estimated at the position of SBB based on

Shapiro and Ritzwoller (2004) – extracted from the SeaRISE project (http://websrv.cs.umt.edu/isis/index.php/Present_Day_Antarctica). Present-day mean annual temperatures on the blue ice area are estimated as $-20\,^{\circ}\mathrm{C}$ based on observations from IMAU AWS 7 which operated from December 1997 to January 2003 (C. H. Reijmer, personal communication, 2010). Since the LGM surface temperatures have varied by about -8 to $+3\mathrm{K}$ (in the Holocene climate optimum) relative to those at present (Sato and Greve, 2012). Surface elevation changes of $250\,\mathrm{m}$ would modify these by only a degree or so, and this range of variability is consistent with stable water isotope variability on the BIA (Sinisalo et al., 2007).

Around 50 stakes have been implanted in the valley and surveyed by various expeditions in the field-seasons 1999/00, 2001/02, 2002/03, 2003/04, 2006/07. Not all stakes were resurveyed and some could not be relocated at all. All stakes were surveyed by differential GPS using a base station tied to a reference marker located on bedrock near the Svea station (Fig. 1). Baselines of less than $20\,\mathrm{km}$ ensured cm relative precision. The largest sources of error were variable stake lean or measurement during windy conditions, however this error was generally much less than the motion of the stakes between surveys over different seasons. Stakes were lost on the high accumulation snow hill between the two BIAs (Fig. 1). For each stake the velocity calculated over the longest available period has been used in our study after checking that the measurements over shorter periods are consistent with the long term trend. Some results published in earlier articles have been improved upon here. Horizontal velocities are very small, the ice is hardly moving in this area compared with ice flow in the surrounding ice sheet. Over large areas of the BIA surface velocities are below $1\,\mathrm{m\,yr^{-1}}$. The stake velocities are shown in Fig. 1 and Table 2. In addition we used some earlier measurements (Ber. Polarforsch. 86, 1991) surveyed using theodolites (see Fig. 1) within one single season that are less reliable than GPS surveys over longer periods.

3 Model

By the nature of its high viscosity, the flow of ice is described by the Stokes equation, which neglects inertia forces and sets the specific driving force, namely density times gravity, $\rho \boldsymbol{g}$, in balance with the divergence of the Cauchy stress, $\mathrm{div}\boldsymbol{\sigma}$,

$$\mathrm{div}\boldsymbol{\sigma} + \rho \boldsymbol{g} = 0. \tag{1}$$

The Cauchy stress tensor, $\boldsymbol{\sigma} = \boldsymbol{\tau} - p\boldsymbol{I}$, can be divided into the deviatoric stress, $\boldsymbol{\tau}$, and, $p = -\mathrm{tr}\boldsymbol{\sigma}/3$, the isotropic pressure.

The standard way of treating ice in glaciers and ice sheets is to assume incompressibility, which is justified if the compression of firn has a negligible influence on the global dynamics of the system. Although in the high accumulation area between the two BIAs firn compaction could have an influence on the local dynamics, in the case of blue ice, where by definition we have no firn layer to account for, this certainly holds and the conservation of mass reduces to

$$\mathrm{div}\boldsymbol{u} = \mathrm{tr}\dot{\boldsymbol{\varepsilon}} = 0. \tag{2}$$

The strain rate tensor $\dot{\boldsymbol{\varepsilon}}$ can be deduced from the velocity vector, $\boldsymbol{u} = (u,v,w)^{\mathrm{T}}$, by

$$\dot{\boldsymbol{\varepsilon}} = \frac{1}{2}\left(\mathrm{grad}\boldsymbol{u} + (\mathrm{grad}\boldsymbol{u})^{T}\right). \tag{3}$$

If treated as an isotropic material, ice rheology is given by a Norton–Hoff power law, with the power law exponent $n = 3$ in Eq. (5) known as Glen's law in glaciology, which collinearily links the deviatoric stress $\boldsymbol{\tau}$ with the strain-rate $\dot{\boldsymbol{\varepsilon}}$:

$$\boldsymbol{\tau} = 2\eta\dot{\boldsymbol{\varepsilon}}, \tag{4}$$

where the effective viscosity η is defined as

$$\eta = \frac{1}{2}(EA)^{-1/n}\dot{\varepsilon}_e^{(1-n)/n}. \tag{5}$$

In Eq. (5), $\dot{\varepsilon}_e^2 = \mathrm{tr}(\dot{\boldsymbol{\varepsilon}}^2)/2$ is the square of the second invariant of the strain-rate tensor. Under applied shear, the ice grains rearrange their c-axes from an a random anisotropic distribution into a more energetically favourable type of fabric (Duval, 2000) and hence the rheology will deviate from isotropic behaviour. To a limited extent, the enhancement factor E can be used to mimic anisotropy effects (Ma et al., 2010). $A = A(T')$ is a rheological parameter which depends on the ice temperature T' relative to the temperature melting point, via an Arrhenius law (Paterson, 1994).

The temperature is obtained from the general balance equation of internal energy and reads

$$\rho c_v \left(\frac{\partial T}{\partial t} + \boldsymbol{u} \cdot \mathrm{grad} T \right) = \mathrm{div}(\kappa \mathrm{grad} T) + \dot{\boldsymbol{\varepsilon}} : \boldsymbol{\sigma}, \tag{6}$$

where $\kappa = \kappa(T)$ and $c_v = c_v(T)$ are the heat conductivity and specific heat of ice, respectively. The last term in the heat transfer equation represents the amount of energy produced by the viscous deformation, which because of the low shear rates in our application has no significant contribution and hence is neglected.

The complete set of equations is solved using the Finite Element Method (FEM) using the open source software package Elmer/Ice (Gagliardini et al., 2013; http://elmerice.elmerfem.org), which has already been applied to glacier simulations of different kinds (Zwinger et al., 2007; Zwinger and Moore, 2009; Zhao et al., 2013), and we use similar numerical settings as discussed in Martín and Gudmundsson (2013).

The age Ψ of the ice is governed by the advection equation

$$\frac{\partial \Psi}{\partial t} + \boldsymbol{u} \cdot \mathrm{grad} \Psi = 1. \tag{7}$$

Because of its purely advective nature, we chose to solve Eq. (7) using a semi-Lagrangian scheme integrated over a period of up to 15 000 yr using the steady state velocity field obtained with a thermo-mechanically coupled solution. Exactly the same semi-Lagrangian method was first applied and explained by Martín and Gudmundsson (2013). In Sect. 5 we chose to present results taken after 15 000 yr, as this corresponds to the timespan since the middle of the last deglaciation in Antarctica (EPICA community members, 2004).

3.1 Anisotropic rheology

Until recently, anisotropy in Elmer/Ice was restricted to the linear General Orthotropic Flow Law (GOLF Gillet-Chaulet et al., 2006) or a co-linear CAFFE model based on an anisotropic Flow Enhancement factor (Seddik et al., 2008, 2011). In more recent work (Martín et al., 2009; Ma et al., 2010), the orthotropic law has been extended to a non-linear form by adding an invariant in the anisotropic linear law. As we will show later, one of our main findings was the necessity to introduce anisotropic flow behavior to understand the ice dynamics of the Scharffenbergbotnen valley and match it qualitatively with the combined data of observed velocities, surface mass balance and surface age distributions. We did this by applying the model introduced and discussed in detail by Martín and Gudmundsson (2013). Then the non-covariant formulation of anisotropic flow Eq. (4) becomes a general tensor relation, which in index notation can be written as

$$\tau_{ij} = 2\eta_{ikjl}\dot{\varepsilon}_{kl}. \tag{8}$$

The 36 independent components of the viscosity tensor $\boldsymbol{\eta}$ are functions of the polycrystalline fabric. Mathematically, this dependency is expressed in terms of the second and fourth order orientation tensors $\boldsymbol{a}^{(2)}$ and $\boldsymbol{a}^{(4)}$, respectively, defined as

$$a^{(2)}_{ij} = < c_i c_j > \text{ and } a^{(4)}_{ijkl} = < c_i c_j c_k c_l >, \tag{9}$$

with $\boldsymbol{c}$ being the c-axis unit vector and $<>$ the volume average. In order to express the fourth order tensor in terms of the second order tensor (Advani and Tucker, 1990), a closure relation is provided (Chung and Kwon, 2002; Gillet-Chaulet et al., 2006).

3.2 Boundary and initial conditions

The governing equations have to be accompanied by boundary conditions for the field variables. All our simulations are performed on a fixed geometry, reducing the otherwise transient kinematic free surface condition

$$\frac{\partial z_\mathrm{s}}{\partial t} + u_\mathrm{s}\frac{\partial z_\mathrm{s}}{\partial x} + v_\mathrm{s}\frac{\partial z_\mathrm{s}}{\partial y} - w_\mathrm{s} = a_\mathrm{s}, \tag{10}$$

to

$$\frac{\partial z_\mathrm{s}}{\partial t} = 0, \tag{11}$$

and consequently rendering the surface net accumulation, a_s, to be part of the solution of the system rather than an additional boundary condition to it. By neglecting atmospheric pressure gradients and shear forces exerted by the atmosphere, the dynamic boundary condition at the free surface reduces to a vanishing Cauchy stress vector,

$$\boldsymbol{t} = \boldsymbol{\sigma} \cdot \boldsymbol{n} = \boldsymbol{0}, \quad z = z_\mathrm{s}(x,t), \tag{12}$$

where $\boldsymbol{n}$ is the outward pointing surface normal,

$$\boldsymbol{n} = \left(-\frac{\partial z_\mathrm{s}}{\partial x}, -\frac{\partial z_\mathrm{s}}{\partial y}, 1\right)^T \Big/ \left\| \left(-\frac{\partial z_\mathrm{s}}{\partial x}, -\frac{\partial z_\mathrm{s}}{\partial y}, 1\right)^T \right\|. \tag{13}$$

The remaining variables to be set at the free surface are the present annual mean temperature – taken to be $T_{z_\mathrm{s}} = -20\,^\circ\mathrm{C}$ – as well as the age of the downwards advected ice

$$\Psi = 0, \quad z = z_\mathrm{s}(x,t). \tag{14}$$

Because of the special hyperbolic nature of Eq. (7), this condition is set only if $\boldsymbol{u} \cdot \boldsymbol{n} < 1$. In other words, only if the velocity is pointing into the glacier, do we set Eq. (14).

Even with the relatively large heat flux of $q_\mathrm{geo} = 60\,\mathrm{mW\,m^{-2}}$ we used, only a small area of the bedrock, beneath the deepest ice at the very outer end of the valley (where it has minor impact on the inner BIA dynamics), reaches pressure melting point. This allows for setting a fixed boundary condition, $\boldsymbol{u} = \boldsymbol{0}$, for the velocity at the bedrock. This, in consequence, prohibits a steady state solution of Eq. (7), as it would lead to infinite age, $\Psi \rightarrow \infty$, at the bedrock. As an initial condition for the age distribution, $\Psi(\boldsymbol{x}, t=0)$, we assumed plug-flow and applied the analytic solution of Lliboutry (1979) using a constant artificial melt-rate of $1.0 \times 10^{-6}\,\mathrm{m\,yr^{-1}}$ to allow for steady state conditions to be applied.

4 Simulation setup

The velocity field resulting from the Stokes equation is an instantaneous response to a given viscosity distribution and not directly influenced by temporal changes of the geometry. On the other hand, temperature and fabric evolution as well as the age/depth distribution depend on the flow history of the glacier and would demand a transient simulation starting from the LGM and extending to the present day. In particular, by our simulations it turned out that the age/depth distribution – even for fixed geometry – is not in a steady state and by the purely convective nature of Eq. (7) demands a transient approach even starting from before LGM to get the correct initial age/depth distribution. Such a simulation demands:

- the LGM geometry (initial condition for z_{s}),
- the LGM age and fabric distribution, Ψ_{LGM} and $a^{(2)}_{ij,\mathrm{LGM}}$ (or spin-up simulation starting one glacier cycle earlier),
- the accumulation/ablation pattern during the whole simulation ($a_{\mathrm{s}}(\boldsymbol{x},t)$ in Eq. 10),
- the surface temperature history from LGM to present $T_{\mathrm{s}}(\boldsymbol{x}_{\mathrm{s}},t)$.

As only limited geomorphological information on LGM geometry is available (Näslund et al., 2000; Hättestrand and Johansen, 2005), at least the first two of these items are largely undetermined. Additionally the computational effort required to run a full-Stokes model for such a long period, with relatively unconstrained geometrical evolution renders a prognostic simulation from LGM a highly unrealistic approach. Consequently, we focused our efforts on studying the effects of anisotropy on ice dynamics within the fixed present day geometry assuming a steady thermal state and prescribed fabrics.

For all simulations we assume steady state ice-flow conditions and calculate the evolution of the age-distribution from a typical ice-sheet configuration to a blue-ice area. To that end, we calculate the steady-state temperature and flow distribution under the present conditions. Using the velocity solution from the steady state run, the age Eq. (7) is integrated from an initial vertically layered plug-flow distribution using a transient run, which – motivated by the values of the most reliable age measurements at the surface – starts at 15 kyr BP.

Based on the data sets presented in Sect. 2, a two-dimensional, unstructured footprint-mesh, covering the glaciated area of SBB in the horizontal plane was created using the open-source meshing software Gmsh (Geuzaine and Remacle, 2009). Horizontal resolution is 30 m in our main region of interest (close to the ice cores), 50 m in the rest of the valley and up to 100 m closer to the boundaries. We extruded this mesh in the vertical direction in 13 levels. The resulting mesh has about 61 000 nodes that are connected in 54 000 linear elements.

Elmer/Ice uses the Finite Element Method to discretize the governing equations. The resulting system matrices for the solution of the temperature field as well as the Stokes equation (velocities and pressure) are pre-conditioned with an incomplete LU decomposition and thereafter solved using the Generalized Conjugate Residual (GCR) method. Because of the non-linearities introduced by the material parameters (heat conductivity and capacity as well as viscosity) each solver for itself has to iteratively solve a linearized system, obtained by a fixed-point iteration for resolving these nonlinearities. Due to their mutual coupling we also have to iteratively solve for temperature and the Stokes equation to obtain a converged solution for the steady state.

Three different setups were tested to study the principal influence of anisotropic rheology on the flow and the age/depth distribution:

(i) *Isotropic* flow using Glen's flow law.

(ii) A *depth-dependent*, piecewise linear *anisotropic* fabric distribution starting from isotropic and developing towards a single maximum fabric towards the bedrock, i.e.

$$a_{11}^{(2)}(h,d) = a_{22}^{(2)}(h,d) = \max\left(1/3(1-2d/h),0\right); \quad a_{33}^{(2)} = 1 - a_{11}^{(2)} - a_{22}^{(2)}, \tag{15}$$

with the local ice thickness $h(x,y)$ and the distance from the free surface, d.

(iii) An over the depth fixed *single maximum anisotropic* fabric:

$$a_{11}^{(2)} = a_{22}^{(2)} = 0; \quad a_{33}^{(2)} = 1. \tag{16}$$

Note that Eq. (15) is defined for three-dimensions, and also applied for the flow-line model. The isotropic and the single maximum case define the extreme configurations of the fabric that may occur and comparison with measured values will show how pronounced the orientation of the c-axis is to be expected.

5 Results

This section presents the numerical simulations we conducted. First, we present the isotropic, three-dimensional (3-D) case, which leads to the problems of having too high horizontal velocities in combination with a far too old ice at the measured ice core positions (see Sect. 2). We attempted to adjust the ice viscosity to produce a reasonable match to observations by globally tuning the enhancement factor, E, in relation (5) as well as changing the internal temperature distribution – and thereby the rate factor, $A(T')$, in Eq. (5). We did this by varying the surface temperature using the constraints given by climate history within realistic values and the geothermal heat flux. However, it was clear that we could not resolve the velocity and age issue. Figure 3 summarizes the characteristics of the flow field computed for different altered parameters in the isotropic flow law (enhancement factor, temperature and mechanical boundary conditions). To that end, we sampled surface velocities of the inner BIA (see Fig. 1), took the average for the absolute values of horizontal and vertical velocity as well as the horizontal components and normed them by the corresponding values of the reference run (isotropic rheology with enhancement factor 1). From this it is clear that the related changes obtained with variations of enhancement factors or boundary conditions in an isotropic setup are only able to alter the magnitude of all components simultaneously. Additionally, only strongly reduced enhancement-factor of $E = 0.1$ would lead to horizontally velocities sufficiently small to match their measured order of magnitude. From Fig. 4 it is clear that there has to be a differentiation for the horizontal components of the velocity, in order to match the directions. Furthermore, the discrepancy of the computed surface mass balance with respect to the measured (see Table 3) for the *isotropic* as well as the *depth-dependent* case indicate that also the vertical surface velocity component has to adapt in a non-isotropic way.

The most plausible remaining explanation for the mismatch of simulated and observed velocities is the *existence of a developed ice-fabric* that alters resistance to flow differently in horizontal and vertical direction.

5.1 Simulations using isotropic rheology in 3-D

The first attempt to model the three-dimensional flow at SBB was to deploy the standard isotropic Glen's flow law (Paterson, 1994). As errors in the digital elevation model can strongly influence the steady state velocity field (Zwinger and Moore, 2009), a short prognostic run allowing for the free surface to adjust for these errors was made. Since no major adjustments of the free surface were observed we chose to use the unaltered geometry for the thermo-mechanically coupled steady state simulations. We use the resulting velocity field and the semi-Lagrangian method to integrate the age advection Eq. (7) over a time span of $15\,\mathrm{kyr}$.

The result of this run is presented in Figs. 4 and 5. Comparing this with the measured velocities (Fig. 1 and Table 3) it is immediately clear that simulated values of horizontal surface velocities exceed measured ones by almost one order of magnitude, and deviate considerably in direction in some places. Simultaneously, the simulated age distribution does not match the measured dates (see Table 1 and Fig. 2). They neither match the absolute values – they are far too old – nor in terms of the relative distribution – the gradient between the positions of the two most reliable measured values is much too large.

For this and all following 3-D runs we further compute the corresponding surface accumulation distribution, a_s, by setting $\frac{\partial z_\mathrm{s}}{\partial t} = 0$ in (10) and using the diagnostically computed velocity field $(u_\mathrm{s}, v_\mathrm{s}, w_\mathrm{s})^\mathrm{T}$ as well as the given surface geometry, z_s. Results of this comparison are listed in Table 3, from which it is clear that, in terms of the reconstructed computed surface mass balance, results obtained with *isotropic* rheology in places are off by multiple orders of magnitudes.

5.2 Simulations using prescribed fabrics in 3-D

In order to investigate the possible influence of anisotropic fabric on the flow inside SBB valley, we altered the three-dimensional setup of SBB prescribing the anisotropic distributions Eqs. (15) and (16), respectively. The results are depicted in Figs. 6, 7 and 8.

The surface velocities in case (ii) with *depth-dependent anisotropic* fabric (Fig. 7a) are insignificantly different from the *isotropic* case (see Fig. 4). The issue of too high velocities (by an order of magnitude) with ill matching directions remains. Also the surface age distribution (Fig. 8a) resembles the one obtained with the *isotropic* flow law (see Fig. 4).

A clear change is observed with case (iii) the *single maximum anisotropic* fabric. The velocities (Fig. 7b) are greatly reduced with respect to the *isotropic* case and now match the directions, with absolute values slightly lower than observed magnitudes. Deeper in the ice, the isochrones become more horizontally aligned, shortening the distance an ice particle has to travel from the accumulation area to the inner valley. For the inner BIA this results in a shifting of the old ice towards the lower end of the valley and hence – at least qualitatively – improving the match with the observed age distribution. The slightly too slow velocities lead to almost stagnant ice down the valley (stake Bi1 in Fig. 1), resulting in too old ice ages there (Fig. 8b). A similar trend can be observed for the computed surface mass balance (SMB). A comparison between the values for the SMB in Table 3 shows a strong reduction of the compared to measured values by order of magnitude too large negative values for the *isotropic* and *depth-dependent* fabric computations.

The change between the *isotropic/depth-dependent anisotropic* and the *single maximum anisotropic* case is even more clearly to be seen in the corresponding 3-D stream-lines. To that end we ran a stream-line solver (Runge–Kutta) provided within ParaView (Ahrens et al., 2005) backwards from a line at the surface that connects the sample-points H and V (see Fig. 1 and Table 1) in order to visualize the origin of ice particles that reach the surface in that region. The results of these post-processing steps are shown in Fig. 9. For the *isotropic* and *depth-dependent anisotropic* fabric cases, the origin of most particles is either from the region between the two BIAs areas or the southern flank on the other side of the surface moraine in the inner part of the valley (depicted in Fig. 1), which in itself already is a a very unrealistic result (as stream-lines are not expected to cross surface moraines). This picture changes for the *single maximum anisotropic* fabric distribution, where all stream-lines are shifted to originate from areas close to the bedrock from within the outer part of the valley, more resembling the contours of our flow-line used for the initial studies. Another clear distinction between the two configurations is the integration time, i.e., the travel time of a particle as a result from the Runge–Kutta method to advect a particle from the surface along the stream-line back to that particular position. Naturally, given the faster velocities, these travel times are much faster for the *isotropic/depth-dependent anisotropic* than the *single maximum anisotropic* fabric, with the latter quickly exceeding 50 000 yr once reaching the outer part of the valley.

5.3 Comparison of 3-D results with 2-D flow line model

In addition to the complete three-dimensional setup, we also investigated the dynamics using a flow-line model, as there have been earlier attempts to compute the age-distribution with such models (Grinsted et al., 2003). Initially chosen to reduce the complexity and the size of the problem, the two-dimensional (2-D) flow-line model illustrates the necessity of using a full three-dimensional flow simulation.

Comparing Fig. 10 and Fig. 6 (first and last row), shows that the results differ quantitatively for both extreme scenarios, the *isotropic* and the *single vertical maximum* fabric. The upwelling region of old ice around 5.5 km along the flow-line observed in the 3-D *isotropic* simulations in case of the *single maximum* fabric is shifted downstream, but maintained in the simulation with *single fabric* in 2-D, while it disappears in 3-D. This leads to a different structure of age distribution in our main region of interest between the points V and H. Also the horizontal velocity for the *single vertical maximum* scenario produces a completely different qualitative distribution from the 3-D case. Higher velocities are observed much further inside the valley (larger distances along the flow-line) with the single fabric, while the simulations with the isotropic fabric are fairly similar (at least for distances beyond the outer first kilometre).

6 Discussion

We presented simulations with an isotropic and two different ad-hoc prescribed fabric distributions: a *depth-dependent* distribution (evolving from isotropic at the surface to a vertical single maximum at one-third of the flow depth); and a uniform *single vertical maximum* fabric. The latter leads to a qualitatively correct reproduction of observed velocities at the BIA.

We get a similar picture from a comparison of the computed surface mass balance. Even if a possible contribution by transient evolution of the ice thickness in our simulations is neglected by the fixed surface, Table 3 makes clear that the *isotropic* as well as the *depth-dependent* fabric mass balance estimates exceed measured surface mass balance values at some places by more than an order of magnitude. Despite not obtaining a perfect match with observed data, in general, the prescribed *single vertical maximum* fabric is the only one that resolves the paradox of lowering the horizontal and the vertical velocities in a non-uniform way.

Since the anisotropic nature of ice introduces very strong differences in ice viscosity relative to the c-axis of the ice crystal, introducing anisotropic fabric provides a plausible solution to the need to reduce flow speed in horizontal and vertical direction in a non-isotropic way. Other possible factors that would locally alter the ice viscosity, such as water content, ice impurities or damage tend to soften the ice (Paterson, 1994) and increase the velocity, and consequently cannot explain the deviation from modeled isotropic velocity with respect to the observed at SBB. Since the blue ice areas are unusual in that the annual layers are tilted (varying from sub-horizontal near the equilibrium line to near vertical at the closed end of the ablation area), the fabric evolves over time and space. The full evolution of the fabric would have to take into account the non-steady state evolution of the SBB valley since the LGM. During the LGM most of the valley was an accumulation region (Hättestrand and Johansen, 2005), and the blue ice was only formed as the surrounding ice sheet surface lowered and the mountain geometry created conditions suitable for effective removal of surface snow and firn (Malm, 2012).

We could not simulate such a dynamic evolution of the valley given the considerable uncertainty of the date and timing of the ice sheet change that then drives the blue ice area evolution, and of course such a long time prognostic run would be prohibitively expensive in computer resources. The flow line case suggested that both a depth varying fabric and a pure single maximum fabric would result in improvements to fit to observed velocities. In the three-dimensional simulation the *depth-dependent fabric* prescription (case (ii)) does not provide a satisfactory fit, while the *single vertical maximum* prescription (case (iii)) performs much better. The *single vertical maximum* fabric assumption certainly is too extreme a scenario and consequently leads too low surface velocities. The real fabric distribution will be spatially varying and our cases (i) - (iii) just provide a spectrum of the most extreme configurations. Nevertheless, the clear trend towards reducing the value and adjusting the directions of the horizontal velocity components while still matching the vertical ones (reflected in matching SMB numbers) give reason to claim that a pronounced fabric at the BIA of Scharffenbergbotnen remains the most likely explanation to correct the significant discrepancy between with isotropic rheologies computed and measured results.

From the comparison of the 2-D with the 3-D results for the age and the velocity in Fig. 10, it is clear that due to the complexity of the flow field, a full 3-D simulation is needed to capture all features. This is confirmed by the twisted distribution of the streamlines depicted in Fig. 9.

It should be pointed out that there are some uncertainties in age observations, especially of ages in the valley. Some of the older measurements were made with a technique based on the ^{14}C age of gas trapped in air, and this is known to be subject to error caused by in-situ production of ^{14}C by cosmic rays that penetrate surface ice layers (van der Kemp et al., 2002). Newer data come from measurements on particles that seem more reliable (Jenk et al., 2006), so there is relatively few data to constrain the model ages.

Our modeling results, in particular the difference between the prescribed *depth-dependent* and *single vertical maximum* fabric, suggest the presence of a strongly anisotropic ice-fabric in SBB not only towards the bottom of the ice column but also near the surface. Considering that the ice-fabric at a particular position not only depends on the local strain-rates but also on the history of previous strain-rates, our results indicate that the strongly anisotropic ice that typically appears in subsurface ice has been advected towards the surface of the BIA.

Strong fabric development has been observed in ice-cores close to the surface (Svensson et al., 2007). Radar studies also that show the presence of strong fabric development near the surface is widespread in Antarctica (Matsuoka et al., 2012). The existence of such a strong anisotropy in ice-fabric is explained by previous modelling results, that show that under compression, extension and shear, flow-induced anisotropy is developed in a fraction of the advection time-scale, ice-thickness divided by vertical velocity, that is a fraction of tens of thousands of years in SBB (Martín and Gudmundsson, 2012). We have not modelled here the evolution of the ice-fabric mainly because of the lack of data but our results support the idea that fabric evolves as rapidly in a BIA as in other areas with different ice-flow characteristics. This could be tested by collection of samples in the blue ice field, however this has never been done at SBB. Indeed such measurements should be made if flow modeling is to be used to help interpret horizontal ice cores.

7 Conclusions

We investigated the ice dynamics of SBB using a full-Stokes flow model, as a tool to aid the interpretation of ice collected for paleoclimate research. We find that using standard isotropic ice fabric results in too high surface velocities and too low vertical ones, making a very poor match with observations of surface age and motion. While it is possible that an in time non-linear thinning of the surface inside the valley since the LGM may contribute to this discrepancy, the present day velocity field should be purely a function of the present day geometry and surface mass balance field. Attempts to vary viscosity using plausible ranges of geothermal heat flux and surface temperature changes since the LGM could not resolve this issue. All other reasons for a drastic change of the velocity field with respect to the isotropic rheology solution may be dismissed as implausible, hence the only remaining explanation for the observed velocities is the existence of pronounced anisotropic fabric.

We cannot provide a transient forcing of the free surface and the fabric evolution since the LGM, however we look at extreme configurations of the rheology for a fixed geometry in SBB. The best match with the observed velocity field was obtained with a fabric showing single vertical maximum. As anisotropy appears to be a key-factor in explaining the observed flow and age/depth distribution at SBB (and probably also in other blue ice areas), we suggest to investigate future ice samples not only with respect to chemistry, but also with respect to the orientation of fabric.

The remaining discrepancies concerning the match between the few reliable observed and computed ages at the surface certainly can be linked to the transient behaviour of the age/depth profile. Even with a fixed geometry and prescribed fabric and temperature distribution (which is equivalent to a given viscosity), no steady state of the age profile can be obtained, neither in 2-D nor 3-D simulations. Our simulated surface age in the inner part of the valley in any configuration is close to the integration time and the maximum observed age at the surface in the innermost blue ice area is about 15 ka. This suggests that the BIA was formed around that time which is plausible given the surface lowering that would have occurred in the ice sheet during the deglaciation.

This is the first time that the importance of anisotropy in the ice dynamics of a blue ice area has been assessed. We show that the understanding of ice anisotropy is key in order to decipher the paleoclimatic records of blue ice areas.

Acknowledgements. This work has been funded by the Finnish Academy (Suomen Akatemia) under the project *Dynamical evolution of Scharffenbergbotnen blue ice area since the Late Glacial Maximum*. We thank A. Grinsted (Centre for Ice and Climate, NBI, Univ. Copenhagen, Denmark) and A. Sinisalo (Univ. Oslo, Norway) for their insightful help on topics concerning their earlier work at SBB. We are grateful to C. H. Reijmer (Institute for Marine and Atmospheric research, Utrecht University, the Netherlands) for providing us with the data from AWS 7. We thank the two reviewers, Eric Larour and Shin Sugiyama, for their constructive critics that helped to improve the quality of this article.

References

Advani, S. G. and Tucker, G. L.: Closure approximations for three-dimensional structure tensors, J. Rheol., 34, 367–386, 1990.

Ahrens, J., Geveci, B., and Law, C.: ParaView: an end-user tool for large data visualization, in: The Visualization Handbook, edited by: Hansen, C. D., and Johnson, C. R., Elsevier, 2005.

Azuma, N., Nakawo, M., Higashi, A., and Nishio, F.: Flow pattern near Massif A in the Yamato bare ice field estimated from the structures and the mechanical properties of a shallow ice core, Mem. NIPR, 39, 173–183, 1985

Ber. Polarforsch. 86: Die Expedition ANTARKTIS-VIII mit FS “Polarstern” 1989/90, Bericht vom Fahrtabschnitt ANT-VIII/5, 1991

Bintanja, R.: On the glaciological, meteorological, and climatological significance of Antarctic blue ice areas, Rev. Geophys., 37, 337–359, 1999.

Bintanja, R. and Reijmer, C. H.: Meteorological conditions over Antarctic blue-ice areas and their influence on the local surface mass balance, J. Glaciol., 47, 37–50, 2001.

Chung, D. H. and Kwon, T. H.: Invariant-based optimal fitting closure approximation for the numerical prediction of flow-induced fiber orientation, J. Rheol., 46, 169–194, 2002.

Crary, A. P. and Wilson, C. R.: Formation of “Blue” Glacier Ice by Horizontal Compressive Forces, J. Glaciol., 3, 1045–1050, 1960.

Duval, P.: Deformation and dynamic recrystallization of ice in polar ice sheets, in Hondoh, T., ed., Physics of Ice Core Records: 103-113, 2000

EPICA community members: Eight glacial cycles from an Antarctic ice core, Nature, 429, 623–628, doi:10.1038/nature02599, 2004

Gagliardini, O., Gillet-Chaulet, F., and Montagnat, M.: A review of anisotropic polar ice models: from crystal to ice-sheet flow models, in: Physics of Ice Core Records II, Inst. of Low Temp. Sci., Hokkaido Univ, Sapporo, Japan, 149–166, 2009.

Gagliardini, O., Zwinger, T., Gillet-Chaulet, F., Durand, G., Favier, L., de Fleurian, B., Greve, R., Malinen, M., Martín, C., Råback, P., Ruokolainen, J., Sacchettini, M., Schäfer, M., Seddik, H., and Thies, J.: Capabilities and performance of Elmer/Ice, a new generation ice-sheet model, Geosci. Model Dev. Discuss., 6, 1689–1741, doi:10.5194/gmdd-6-1689-2013, 2013.

Geuzaine, C. and Remacle, J.-F.: Gmsh: a three-dimensional finite element mesh generator with built-in pre- and post-processing facilities, Int. J. Numer. Meth. Eng., 79, 1309–1331, 2009.

Gillet-Chaulet, F., Gagliardini, O., Meyssonnier, J., Zwinger, T., and Ruokolainen, J.: Flow-induced anisotropy in polar ice and related ice-sheet flow modelling, J. Non-Newton Fluid, 124, 33–43, 2006.

Grinsted, A., Moore, J., Spikes, V. B., and Sinisalo, A.: Dating Antarctic blue ice areas using a novel ice flow model, Geophys. Res. Lett., 30, 2005, doi:10.1029/2003GL017957, 2003.

Herzfeld, U. C. and Holmlund, P.: Geostatistics in glaciology: implications of a study of Scharffenbergbotnen, Dronning Maud Land, East Antarctica, Ann. Glaciol., 14, 107–110, 1990.

Hättestrand, C. and Johansen, N.: Supraglacial moraines in Scharffenbergbotnen, Heimefrontfjella, Dronning Maud Land, Antarctica – significance for reconstructing former blue ice areas, Antarct.

Sci., 17, 225–236, doi:10.1017/S0954102005002634, 2005.
Jenk, T. M., Szidat, S., Schwikowski, M., Gäggeler, H. W., Brütsch, S., Wacker, L., Synal, H.-A., and Saurer, M.: Radiocarbon analysis in an Alpine ice core: record of anthropogenic and biogenic contributions to carbonaceous aerosols in the past (1650–1940), Atmos. Chem. Phys., 6, 5381–5390, doi:10.5194/acp-6-5381-2006, 2006.
Jouzel, J., Raisbeck, G., Benoist, J. P., Yiou, F., Lorius, C., Raynaud, D., Petit, J. R., Barkov, N. I., Korotkevitch, Y. S., and Kotlyakov, V. M.: A comparison of deep Antarctic ice cores and their implications for climate between 65 000 and 15 000 years ago, Quatern. Res., 31, 135–150, 1989.
van der Kemp, W. J. M., Alderleisten, C., van der Borg, K., de Jong, A. F. M., Lamers, R. A. N., Oerlemans, J., Thomassen, M., and van de Wal, R. S. W.: In situ produced ^{14}C by cosmic ray muons in ablating Antarctic ice, Tellus B, 54, 186–192, doi:10.1034/j.1600-0889.2002.00274.x, 2002.
Lliboutry, L. A.: A critical review of analytical approximate solutions for steady state velocities and temperature in cold ice sheets, Gletscherk. Glacialgeol., 15, 135–148, 1979.
Ma, Y., Gagliardini, O., Ritz, C., Gillet-Chaulet, F., Durand, G., and Montagnat, M.: Enhancement factors for grounded ice and ice shelves inferred from an anisotropic ice-flow model, J. Glaciol., 56, 805–812, doi:10.3189/002214310794457209, 2010.
Malm, T.: Simulation of Wind Fields at Scharffenbergbotnen, Antarctica and their Impact on Blue Ice Areas, master thesis, Aalto University, School of Engineering, available at: http://lib.tkk.fi/Dipl/2011/urn100517.pdf, 2012.
Martín, C., Gudmundsson, G. H., Pritchard, H. D., and Gagliardini, O.: On the effects of anisotropic rheology on ice flow, internal structure, and the age–depth relationship at ice divides, J. Geophys. Res., 114, F04001, doi:10.1029/2008JF001204, 2009.
Martín, C. and Gudmundsson, G. H.: Effects of nonlinear rheology, temperature and anisotropy on the relationship between age and depth at ice divides, The Cryosphere, 6, 1221-1229, doi:10.5194/tc-6-1221-2012, 2012.
Martín, C. and Gudmundsson, G. H.: Modelling of Kealey Ice Rise, Antarctica, reveals stable ice-flow conditions in East Ellsworth Land over millennia, accepted J. Glaciol., 2013.
Matsuoka, K., Power, D., Fujita, S., and Raymond, C. F.: Rapid development of anisotropic ice-crystal-alignment fabrics inferred from englacial radar polarimetry, central West Antarctica, J. Geophys. Res., 117, F03029, doi:10.1029/2012JF002440, 2012.
Moore, J. C., Nishio, F., Fujita, S., Narita H., Pasteur E., Grinsted, A., Sinisalo, A., and Maeno, N.: Interpreting ancient ice in a shallow ice core from the South Yamato (Antarctica) blue ice area using flow modeling and compositional matching to deep ice cores, J. Geophys. Res., 111, D16302,

doi:10.1029/2005JD006343, 2006.
Naruse, R. and Hashimoto, M.: Internal flow lines in the ice sheet upstream of the Yamato Mountains, East Antarctica, Mem. NIPR, 24, 201–203, 1982.
Näslund, J. O., Fastook, J. L., and Holmlund, P.: Numerical modeling of the ice sheet in western Dronning Maud Land, East Antarctica: impacts of present, past and future climates, J. Glaciol., 46, 54–66, 2000.
Paterson, W. S. B.: The Physics of Glaciers, 3 Edn., Pergamon, 1994.
Pattyn, F.: The variability of Antarctic ice-sheet response to the climatic signal, Ann. Glaciol., 29, 273–278, 1999.
Pattyn, F. and Decleir, H.: Ice dynamics near Antarctic marginal mountain ranges: implications for interpreting the glacial-geological evidence, Ann. Glaciol., 27, 327–332, 1998.
Ritz, C., Rommelaere, V., and Dumas, C.: Modeling the evolution of Antarctic ice sheet over the last 420 000 years: implications for altitude changes in the Vostok region, J. Geophys. Res., 106, 31943–31964, doi:10.1029/2001JD900232, 2001.
Van Roijen, J. J.: Determination of ages and specific mass balances from C_{14} measurements on Antarctic surface ice, Ph. D. thesis, Faculty of Physics and Astronomy, Utrecht University, Utrecht, the Netherlands, 1996.
Sato, T., and Greve, R.: Sensitivity experiments for the Antarctic ice sheet with varied sub-ice-shelf melting rates, Ann. Glaciol., 53(60), 221—228, doi:10.3189/2012AoG60A042, 2012
Seddik, H., Greve, R., Placidi, L., Hamann, I., and Gagliardini, O.: Application of a continuum-mechanical model for the flow of anisotropic polar ice to the EDML core, Antarctica, J. Glaciol., 54, 187, 631—664, doi:10.3189/002214308786570755, 2008.
Seddik, H., Greve, R., Zwinger, T., and Placidi, L.: A full Stokes ice flow model for the vicinity of Dome Fuji, Antarctica, with induced anisotropy and fabric evolution, The Cryosphere, 5, 495–508, doi:10.5194/tc-5-495-2011, 2011.
Shapiro, N. M. and Ritzwoller, M. H.: Inferring surface heat flux distributions guided by a global seismic model: particular application to Antarctica, Earth Planet. Sci. Lett., 223, 213–224, doi:10.1016/j.epsl.2004.04.011, 2004.
Sinisalo, A. and Moore, J. C.: Antarctic blue ice areas – towards extracting palaeoclimate information, Antarc. Sci., 22, 99–115, doi:10.1017/S0954102009990691, 2010.
Sinisalo, A., Moore, J. C., van de Wal, R. S. W, Bintanja, R.m and Jonssona, S.: 14 year mass-balance record of a blue-ice area in Antarctica, Ann. Glaciol. 37, pp. 213-218, doi:10.3189/172756403781816013, 2003

Sinisalo, A., Grinsted, A., and Moore, J. C.: Dynamics of the Scharffenbergbotnen blue-ice area, Dronning Maud Land, Antarctica, Ann. Glaciol., 39, 417–423, 2004.

Sinisalo, A., Grinsted, A., Moore, J. C., Meijer, H. A. J., Martma, T., and van de Wal, R. S. W.: Inferences from stable water isotopes on the Holocene evolution of Scharffenbergbotnen blue ice area, East Antarctica, J. Glaciol., 53, 427–434, 2007.

Svensson, A., Durand, G., Mathiesen, J., Persson, A., and Dahl-Jensen, D.: Texture of the Upper 1000 m in the GRIP and North GRIP Ice Cores, in Physics of Ice Core Records II: Papers collected after the 2nd International Workshop on Physics of Ice Core Records, held in Sapporo, edited by: Hondoh, T., Japan, 2-6 February 2007, 2007.

Takahashi, S., Endoh, T., Azuma, N., and Meshida, S.: Bare ice fields developed in the inland part of Antarctica, Proc. NIPR Symp. Polar Met. Glaciol., 5, 128–139, 1992.

Whillans, I. M. and Cassidy, W. A.: Catch a falling star; meteorites and old ice, Science, 222, 55–57, 1983.

Zhao, L., Tian, L., Zwinger, T., Ding, R., Zong, J., Ye, Q., and Moore, J. C.: Numerical simulations of Gurenhekou Glacier on the Tibetan Plateau, J. Glaciol, accepted, 2013.

Zwinger T., Greve, R., Gagliardini, O., Shiraiwa, T., and Lyly, M.: A full Stokes-flow thermo-mechanical model for firn and ice applied to the Gorshkov crater glacier, Kamchatka, Ann. Glaciol., 45, 29–37, 2007.

Zwinger, T. and Moore, J. C.: Diagnostic and prognostic simulations with a full Stokes model accounting for superimposed ice of Midtre Lovénbreen, Svalbard, The Cryosphere, 3, 217–229, doi:10.5194/tc-3-217-2009, 2009.

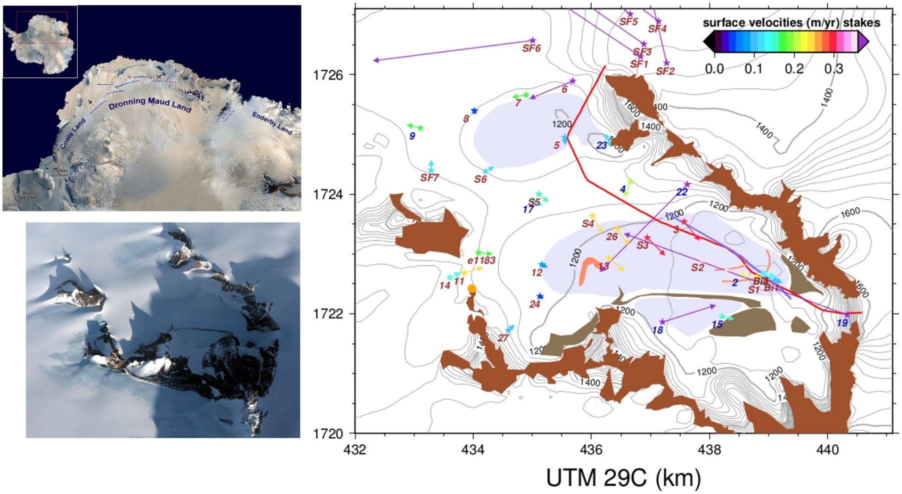

Fig. 1. Satellite pictures indicating the position of Dronning Maud land (credits Wikimedia Commons) and of the Scharffenbergbotnen (SBB) valley (NASA public imagery) and a sketch of the domain augmented with observed stake and GPS velocities. The right sketch shows velocities as arrows annotated by the stake reference code (red are GPS measurements, blue are theodolites) with corresponding stake positions as star and the color according to the velocity legend. GPS velocities are based on surveys using Svea station (large yellow circle) as reference point. Geological and geographical features: brown rocks, dark-gray moraines, light-gray blue ice, orange lines distinctive features within the blue ice, long ice core in blue, position of the vertical transect for the flow-line model (red) within the area of SBB. All coordinates in this figure and also the following figures are defined by WGS84, UTM zone 29C.

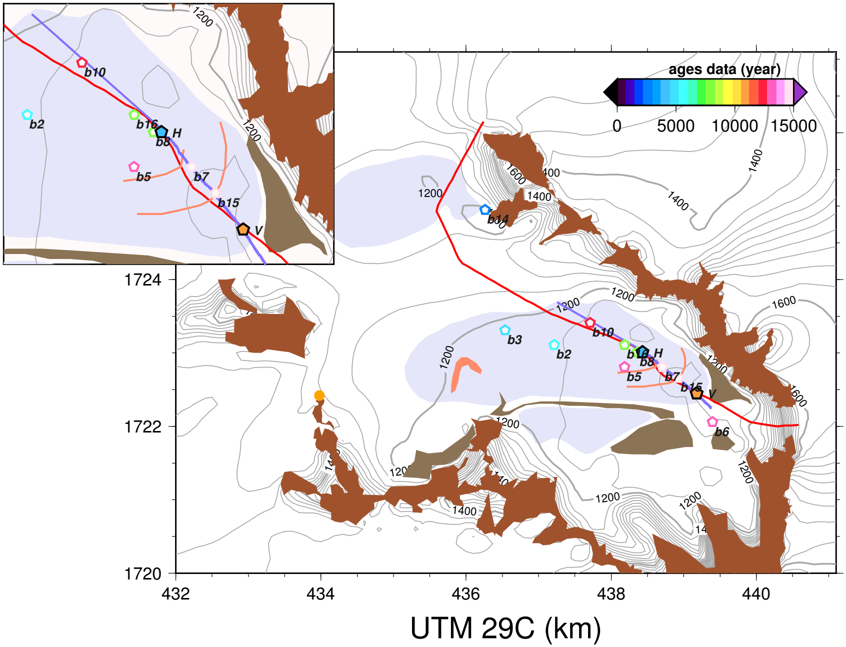

Fig. 2. Sketch of the Scharffenbergbotnen (SBB) valley augmented with measured surface ages. Geological and geographical features are the same as in Fig. 1. The inset on the upper left side is a zoom of the area around the horizontal ice core. Age measurements are shown as pentagons with the coloring according to the age legend with a distinction between reliable data (black line filled with color) and data points with larger errors (colored line empty center) – see Table 1.

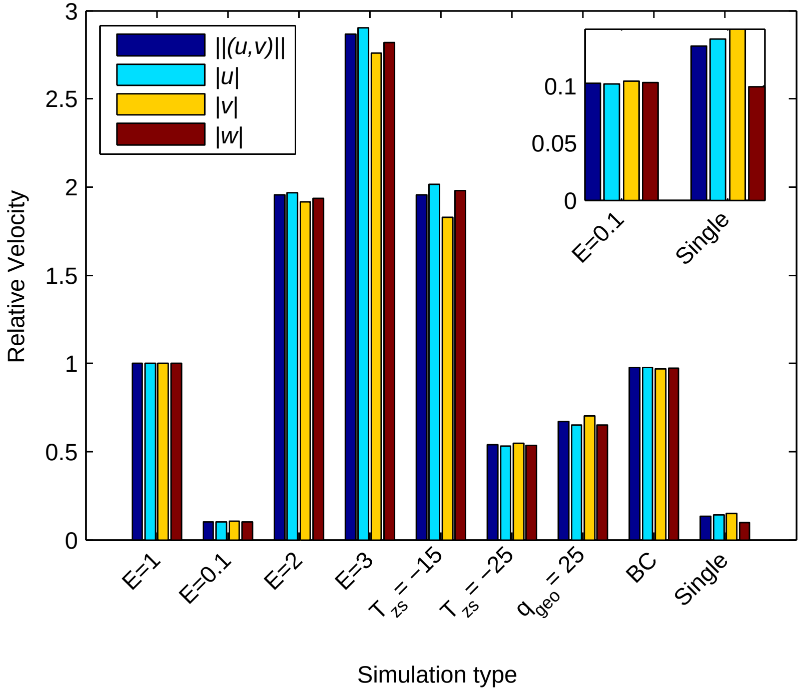

Fig. 3. Summary statistics showing how component magnitudes of the velocity vector $\boldsymbol{u} = (u,v,w)^{\mathrm{T}}$ averaged over the inner BIA field are affected by changes to simulation parameters relative to the values in a standard simulation. Values are relative to simulations using an isotropic flow law (5); enhancement factor, $E = 1$; surface temperature, $T_{\mathrm{zs}} = -20\,^{\circ}\mathrm{C}$; geothermal heat flux, $q_{\mathrm{geo}} = 60$ mW m^{-2} (leftmost 4 columns). The other column sets represent results from simulations with a single parameter varying from this standard configuration as denoted by labels beneath the columns. BC represent a simulation with no inflow, $\boldsymbol{u} = 0$ on the otherwise free inflow boundary of the domain. The rightmost set are results for the single maximum fabric simulation, and the inset emphasizes differences in horizontal and vertical components between this case and the isotropic case with reduced enhancement factor ($E = 0.1$).

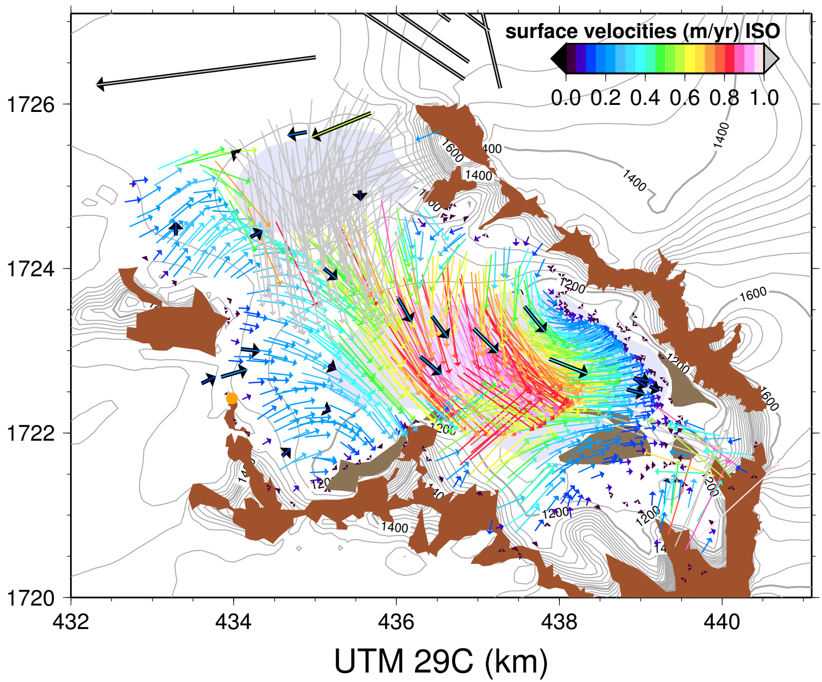

Fig. 4. Horizontal velocity distribution (scale bar) obtained with the isotropic Glen's flow law compared with measured velocities (thick arrows, see Table 2 for values). Discrepancies in both direction and magnitude (with observed velocities being almost an order of magnitude smaller) can be easily seen.

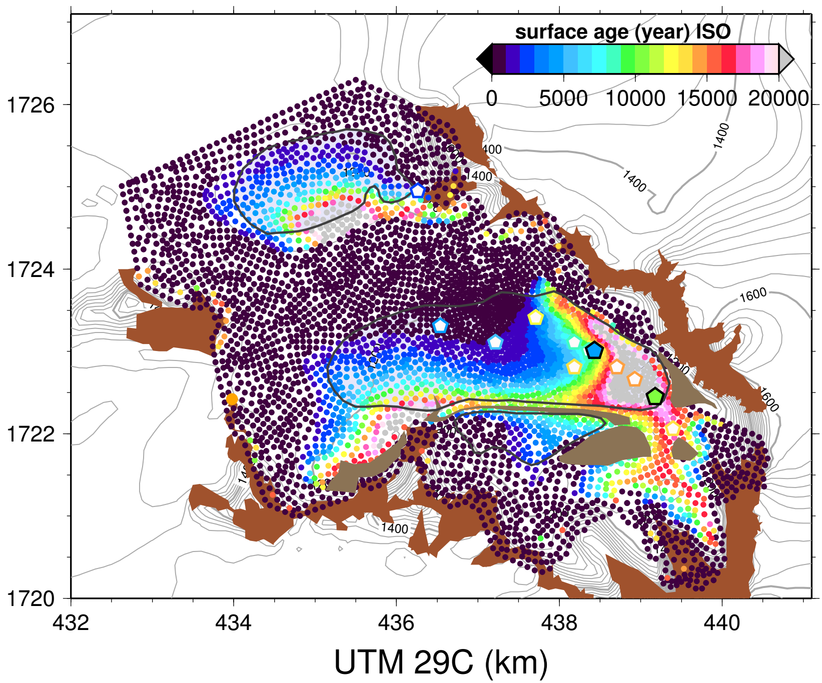

Fig. 5. Age (dots - scale bar) distribution obtained with the isotropic Glen's flow law and a 15 kyr integration of the age equation compared to measured (pentagons). Solid lines enclose BIAs.

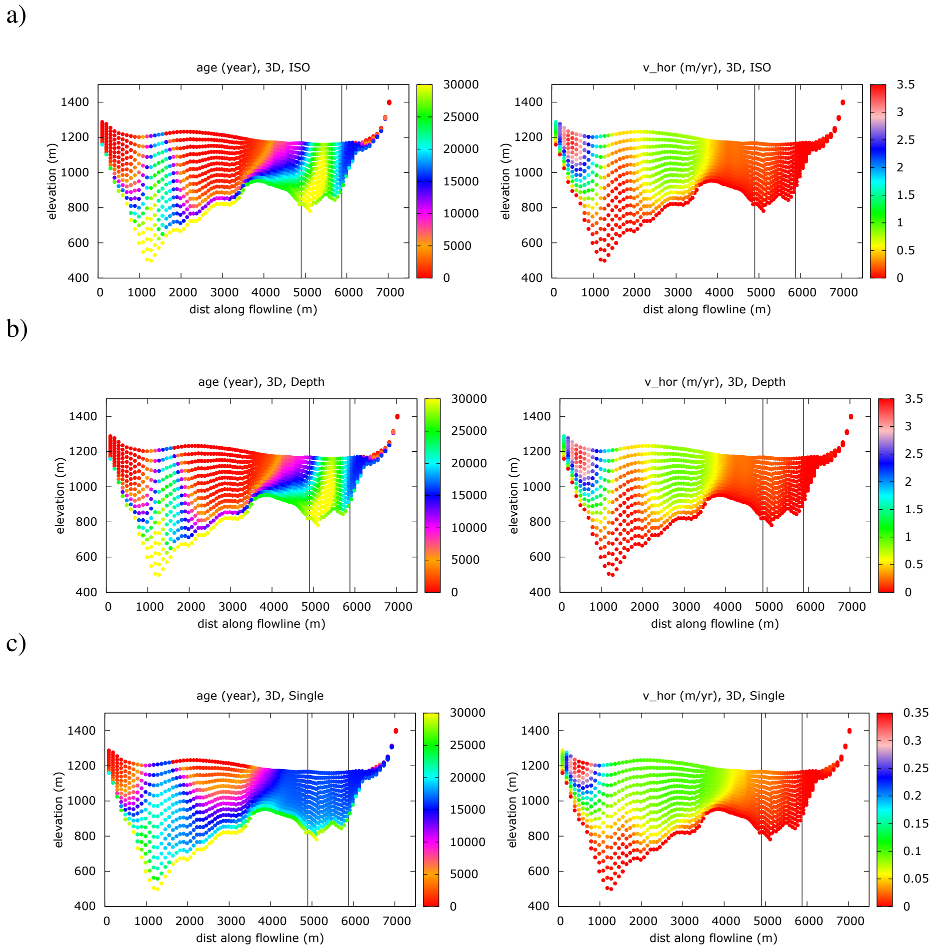

Fig. 6. Comparison of age (left column) and velocity (right column) values obtained on the flow-line (red line shown in Fig. 1) with the three-dimensional model using **(a)** isotropic Glen's flow law, **(b)** depth-dependent fabric and **(c)** single maximum fabric distribution (mind: one order of magnitude lower velocities). Age values are computed applying an integration over 15 kyr. The two vertical lines mark the intersection with the horizontal ice core at points V and H.

Table 1. Measured calibrated ages at the surface including error in comparison to computed ages for the three different prescribed *isotropic* (iso), *depth-dependent* (depth) and the *single vertical maximum* (single) fabrics. The most reliable measurement points, V and H are indicated in bold. Coordinate positions are given in UTM 29C.

site	Easting [m]	Northing [m]	measured [yr]		computed age [yr]		
			age	error	iso	depth	single
b2	437 214.35	1 723 105.09	5978	2627	1108.55	1102.26	11082.22
b3	436 537.15	1 723 307.14	4948	5405	568.55	563.07	5690.62
b5	438 183.76	1 722 806.78	13 166	6883	6632.08	6486.71	16477.31
b6	439 395.07	1 722 064.31	13 479	2842	17872.73	17873.40	15591.90
b7	438 708.77	1 722 806.66	14 574	4390	20462.19	20304.46	16083.52
b8	438 360.77	1 723 006.73	8264	1888	9079.54	8931.84	16140.22
b10	437 710.91	1 723 406.88	12 119	8679	2911.06	2830.00	10717.50
b14	436 262.64	1 724 953.09	2978	1063	2573.93	884.84	6632.62
b15	438 925.77	1 722 656.62	14 975	2884	29080.30	29053.04	16185.09
b16	438 185.76	1 723 106.78	8084	1708	7870.36	7760.71	16144.07
V	439 175.79	1 722 452.40	10 500	500	21212.22	21207.46	15687.64
H	438 432.31	1 723 013.61	4426	215	10889.65	10733.31	16065.01

Table 2. Measured surface velocities. Point sites within the inner BIA are indicated with bold letters. Coordinates are in UTM 29 C.

site	Easting [m]	Northing [m]	$\boldsymbol{u}$ measured $[\mathrm{m\,yr}^{-1}]$
S1	438 828.65	1 722 527.04	0.161
S2	437 876.72	1 722 897.62	0.358
S3	436 949.11	1 723 273.82	0.301
S4	436 018.18	1 723 635.99	0.241
S5	435 111.34	1 723 999.86	0.146
S6	434 203.94	1 724 379.2	0.124
e1183	434 087.58	1 723 023.08	0.174
Bi1	439 107.11	1 722 569.08	0.100
Bi4	438 917.10	1 722 672.78	0.142
Bi5	438 914.97	1 722 673.77	0.145
SF1	436 834.46	1 726 301.26	1.699
SF2	437 274.67	1 726 190.40	2.058
SF3	436 892.27	1 726 509.94	1.863
SF4	437 137.94	1 726 887.94	3.111
SF5	436 657.58	1 727 014.65	3.041
SF6	435 009.84	1 726 569.54	1.900
SF7	433 290.53	1 724 402.85	0.118
3	437 570.43	1 723 537.73	0.291
5	435 548.52	1 724 952.50	0.093
6	435 686.91	1 725 891.61	0.554
7	434 898.37	1 725 657.45	0.171
8	434 022.38	1 725 386.28	0.049
11	433 845.29	1 722 684.43	0.237
12	435 164.38	1 722 815.35	0.080
13	436 293.16	1 722 929.71	0.241
14	433 605.43	1 722 599.62	0.139
24	435 130.99	1 722 293.10	0.052
26	436 436.46	1 723 418.37	0.237
27	434 596.84	1 721 715.66	0.103

Table 3. Measured (Sinisalo et al., 2003) and computed surface mass balance in mm a^{-1} w.e. and comparison between measured and computed surface velocities for the *isotropic* (iso), *depth-dependent* (depth) and the *single vertical maximum* (single) fabric. Compare stake positions with Fig. 1.

StakeNo.	SMB $[\mathrm{mm\,yr}^{-1}]$ 1988–2002	SMB computed $[\mathrm{mm\,yr}^{-1}]$ iso	depth	single	$\boldsymbol{u}$ measured $[\mathrm{m\,yr}^{-1}]$	computed $[\mathrm{m\,yr}^{-1}]$ iso	depth	single
inner BIA								
3	-30± 41	-151	-151	-13	0.291	0.523	0.523	0.082
13	-33± 38	-388	-388	-35	0.241	0.912	0.912	0.101
26	-6± 51	-144	-144	-13	0.237	0.986	0.986	0.108
outside the inner BIA								
5	-8± 62	-1989	-1996	-82	0.093	1.786	1.795	0.150
6	-2± 75	-910	-908	-121	0.554	6.149	6.163	0.571
7	2± 46	-2713	-2733	-98	0.171	5.620	5.653	0.221
8	4± 67	-874	-874	-15	0.049	1.591	1.591	0.060
12	4± 73	-133	-133	-15	0.080	0.347	0.347	0.057
24	-11± 60	-80	-80	-9	0.052	0.239	0.239	0.038
27	14± 87	96	96	7	0.103	0.280	0.280	0.018

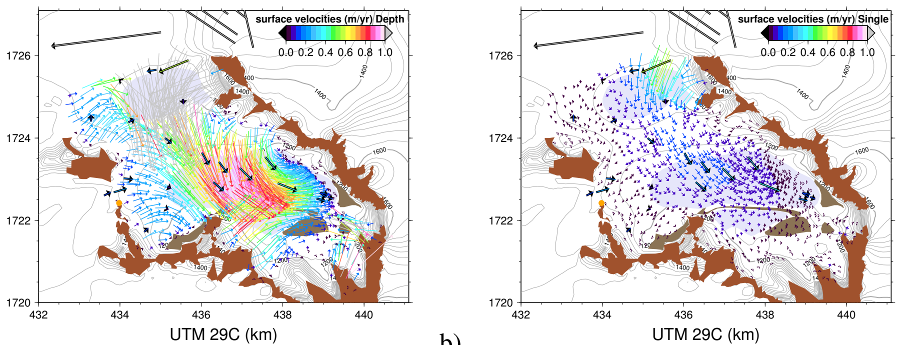

a) b)

Fig. 7. Surface velocity (vectors) for the anisotropic flow law using **(a)** a depth-dependent fabric and **(b)** a single maximum fabric distribution. The surface velocities in the depth-dependent anisotropic case **(a)** are not significantly altered with respect to the isotropic case. However, applying a single maximum fabric reduces velocities (even reducing them too much) and produces better agreement in direction.

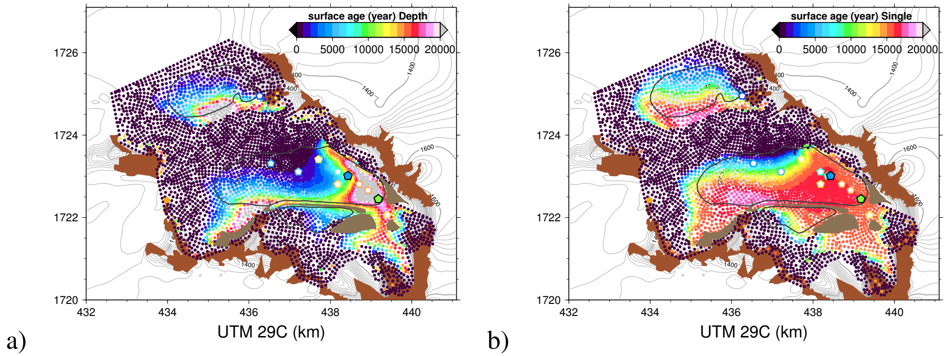

Fig. 8. Age (dots) distribution obtained with the anisotropic flow law using **(a)** depth-dependent fabric distribution and **(b)** single maximum fabric for integration times of 15 kyr.

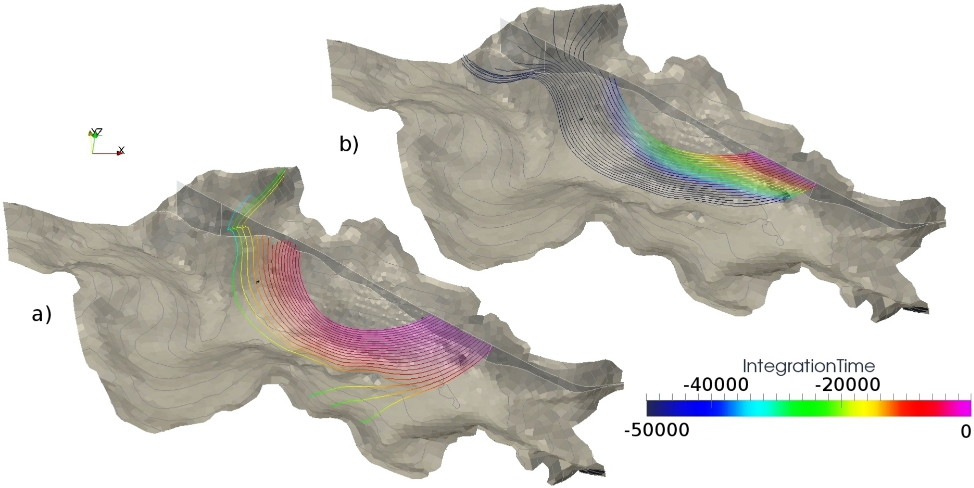

Fig. 9. Streamlines obtained with the backward Runge-Kutta method implemented in ParaView starting from the area where the ice cores have been sampled, colored by integration time given in years **(a)** isotropic and **(b)** single maximum fabric/depth distribution. The depth-dependent anisotropic fabric (not shown) is almost the same as the isotropic case and is characterized by stream-lines originating in the area between the inner and the outer BIA and at the southern flanks. In contrary, the single maximum fabric shifts the origin of the stream-lines towards the outer parts of the valley and significantly increases the travel time of the fluid particles.

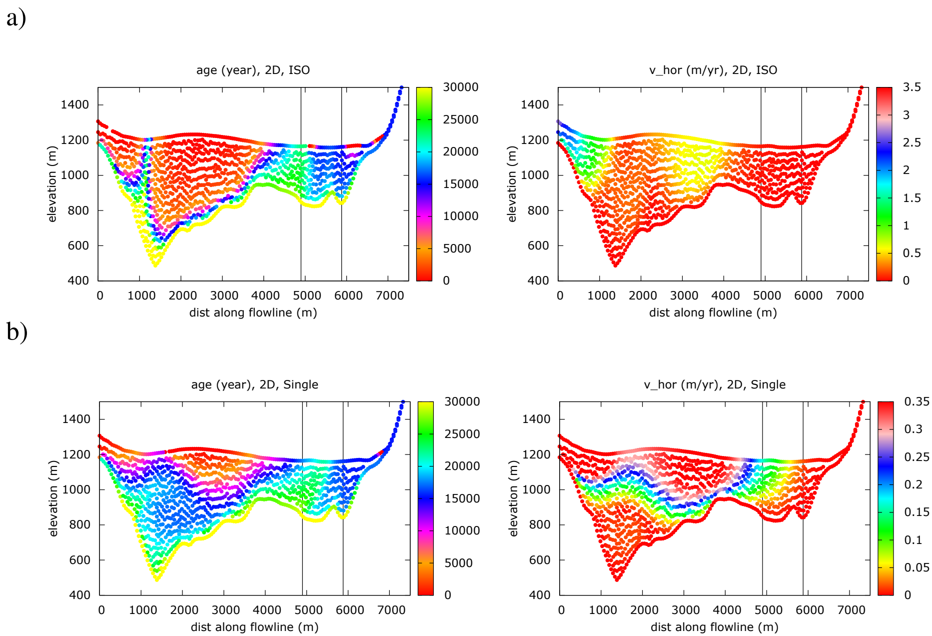

Fig. 10. Ages (left column) and absolute horizontal velocity (right column) of the 2-D flow-line model using **(a)** isotropic Glen's flow law, **(b)** single maximum fabric distribution (mind the different velocity scale). The two vertical lines mark the intersection with the horizontal ice core at points V and H.